Neutron-Resonance Spectroscopy. VIII. The Separated Isotopes of Erbium: Evidence for Dyson's Theory Concerning Level Spacings*

H. I. Liou, H. S. Camarda,† S. Wynchank,‡ M. Slagowitz, G. Hacken, F. Rahn, and J. Rainwater
Columbia University, New York, New York 10027
(Received 6 July 1971)

Results are given for high-resolution neutron-resonance-spectroscopy studies of the separated erbium isotopes (164, 166, 167, 168, 170) using the Nevis Synchrocyclotron. These results, particularly Er^{166} to 4200 eV ($n=109$ levels), give the first excellent agreement with the Dyson-Mehta (DM) Δ statistic which applies for the statistical orthogonal ensemble (O.E.) of Wigner and Dyson. The observed Er^{166} levels seem to be a nearly pure and complete s population, fitting Wigner's nearest-neighbor spacing law and the Porter-Thomas (PT) single-channel Γ_n^0 distribution. The weakest Er^{168} and Er^{170} levels include some p levels (excess of weak Γ_n^0 values) which are separated by a Bayes-theorem method yielding resulting s populations which also give good fits to all statistical O.E. tests. Unexpectedly, the Er^{166} levels give a nonzero correlation coefficient between adjacent Γ_n^0 values of $\rho(\Gamma_{nj}^0, \Gamma_{nj+1}^0) = -0.21 - 0.08$, and with less fluctuation in $\sum\Gamma_n^0$ over adjacent intervals than expected for an uncorrelated PT series of Γ_n^0 values. Assuming a true p level density 3 times that for s levels, S_1 values are calculated on the basis of the observed excess of weak levels and our known level detection threshold. We obtain $10^4 S_0 = 1.70 \pm 0.23$, 1.89 ± 0.20, 1.50 ± 0.21, and 1.54 ± 0.22 for 166, 167, 168, 170; and $10^4 S_1 = \leq 0.75$, 0.70 ± 0.20, and 0.80 ± 0.25 for 166, 168, 170. We find $\Delta = 0.455$ ($n=109$) for Er^{166}, 0.287 ($n=50$) for Er^{168}, and 0.359 ($n=31$) for Er^{170} vs DM's predicted $\Delta = 0.47 \pm 0.11$, 0.39 ± 0.11, and 0.34 ± 0.11. For a large n, Δ is much larger for an uncorrelated Wigner (U.W.) spacing sequence or for an incomplete or impure s level O.E. set. The correlation coefficient for adjacent spacings, $\rho(S_j, S_{j+1}) \equiv \rho = -0.22$, -0.29, -0.09 for 166, 168, 170 vs $\rho \approx -0.27$ (± 0.09, 0.13, 0.17 for 166, 168, 170) (O.E.). The probability is 0.0004 for $[\Delta + \rho] \leq$ the Er^{166}(4.2-keV) value for a U.W. set. The $\langle D \rangle$ values for s levels, if our s level count is correct, are 38.4, 4.06, 95.3, and 155 eV [$\pm 0.9/n$ fractional uncertainty (O.E.)] for $n = 109$, 30, 50, and 31 for 166, 167, 168, 170.

I. INTRODUCTION

This is the eighth of a series[1] of papers presenting the results of high-intensity, high-resolution neutron time-of-flight resonance spectroscopy studies using the Columbia University Nevis synchrocyclotron as a pulsed-neutron source. The results presented in this paper for the separated Er isotopes were mainly obtained during a run in early 1968 when excellent data were obtained for a large number of natural-element and separated isotopes over an effective period of about 8 weeks of 24-h–a-day operation. The authors of this paper spent most of their waking hours during this period maintaining the operation of the over-all experimental system and collecting these data. The data were then divided among the group members for subsequent analysis, with considerable interaction to evolve effective techniques and assure the accuracy of the results. Portions of the analysis required evaluation of systematics involving all of the data. Dr. H. I. Liou had previously analyzed earlier much less satisfactory Er isotope data obtained during 1965 and 1966 (Ph.D. thesis). He was also principally responsible for the analysis of the 1968 Er data. The earlier results were not published, because of the far superior quality of the 1968 data.

These Er results, especially those for Er^{166}, are particularly interesting in that they represent by far the best experimental situation to date where a large population of s-wave neutron resonances has been obtained, essentially free of p-wave contamination and missed s-wave levels. They therefore represent by far the best experimental data to date for tests of the various statistical theories for single populations that have been developed since about 1956. They provide the first excellent test and confirmation of the Dyson-Mehta (DM) predictions[2] for crystalline-lattice-type long- and short-range order in the level spacing distribution. They also provide an excellent test for other theoretical predictions[3] concerning the presence or absence of regularities and correlations between various population parameters such as the nearest-neighbor level spacings and the reduced s-wave neutron widths, as discussed in Paper III.[1]

In addition to presenting our results for the observed neutron-resonance energies, Γ_n^0 values, isotope identification, and (in favorable cases) Γ_γ values for the several hundred analyzed resonances of the Er isotopes for $E \lesssim 10$ keV, we also

give results for the observed s- and p-wave strength functions and the mean s-wave isotope level spacings.

Statistical theories for level spacing systematics, distribution of Γ_n^0 values about $\langle\Gamma_n^0\rangle$, etc., usually assume that a "single level population" is involved. Such levels have the same Z, A, J, and parity, with no "hidden quantum numbers" or "intermediate-structure" modulation of the *a priori* mean values of $\langle\Gamma_n^0\rangle$, etc., over the energy interval studied. The odd-A nuclei tend to be less suitable for such tests, since: (a) They have *two* randomly mixed independent s populations with $J = I \pm \frac{1}{2}$; and (b) the mean level spacing tends to be much smaller, with a lack of Wigner repulsion for nearby states of different J (so levels are more apt to be missed experimentally).

For a single population, previous studies,[1] although of poorer quality, have provided confidence in the essential correctness of Wigner's hypothesis[3] that the nearest-neighbor energy spacings, S_j, are distributed about their mean, $\langle D\rangle$, in the manner

$$P(x)\,dx = \tfrac{1}{2}\pi x e^{-\pi x^2/4}\,dx\,, \tag{1}$$

where $x \equiv S/\langle D\rangle$. The level-repulsion effect is helpful experimentally, since for suitable even-even isotope samples, the difficult problem of resolving almost coincident resonances is much less apt to occur.

For a single population of $l = 0$ resonances, the reduced neutron widths, $\Gamma_n^0 \equiv \Gamma_n(1\text{ eV}/E)^{1/2}$, have been shown to obey the Porter-Thomas (PT)[4] single-channel distribution. In the R-matrix theory,[5] Γ_n^0 is proportional to $\gamma_\lambda{}^2$ for a given level λ, where γ_λ corresponds to channel boundary amplitudes for an appropriately constructed set of normalized system eigenstates (quasibound states). The essential idea is that the individual γ_λ should have a Gaussian distribution about a zero mean, with a variance proportional to $\langle\Gamma_n^0\rangle$ for the population. The result is a several orders of magnitude range of Γ_n^0 values for a single population of ~100 adjacent levels:

$$P(y)\,dy = (2/\pi)^{1/2} e^{-y^2/2}\,dy\,, \tag{2}$$

where $y = (\Gamma_n^0/\langle\Gamma_n^0\rangle)^{1/2}$. A single even-even ($I = 0$) isotope target, having a favorable average s-level spacing $\langle D\rangle$ for measurement, is desirable for obtaining a large sample single s-level population. *A priori*, U^{238} and Th^{232} seemed to be good cases (Paper III[1]), but the separation of weak s levels from p levels and/or spurious "levels" seems not to have been done well. (The U^{238}, Th^{232} cases are reconsidered in the accompanying paper.[6]) The general problem is as follows. One expects ~3 times the density of p levels as s levels, where the Γ_n strengths for the p levels average smaller than those for s levels by a factor $(S_1/S_0)(E/E_1)$, where E_1 (≈350 keV for Er) is the energy where the neutron $\lambda\!\!\!^{-} =$ the effective nuclear radius R. The s strength function S_0 is defined as

$$S_0 = \langle\Gamma_n^0\rangle/\langle D\rangle = \sum_j \Gamma_{n\,j}^0/\Delta E\,, \tag{3}$$

for the energy interval ΔE studied, and S_1 is defined as in Paper III.[1]

The peaking of Eq. (2) for small Γ_n^0 is such that the following probabilities apply: That $\Gamma_n^0/\langle\Gamma_n^0\rangle$ be ≤ 0.01 (8%), ≤ 0.001 (~3%), ≤ 0.0001 (0.8%), while $(E/E_1) \gtrsim 0.01$ at the upper end of the energy regions where we detect and resolve essentially all s levels. The most favorable test nuclei have $150 \lesssim A \lesssim 190$. This is the region of the quadrupole split giant $4s$ "size-resonance" peak in S_0, but where S_1 is small at low E. The situation is less favorable for the Th^{232}, U^{238} region, and very poor for the nuclei having $A = 75$ to 135 that we studied in our Papers IV, V, and VI.[1]

The samples studied during the 1968 run include many even-even isotopes in the range of the $n = 4$ peak in S_0. The erbium results provide the best test case and are being reported first in this paper.

II. EXPERIMENTAL SYSTEM DETAILS FOR THE 1968 MEASUREMENTS

The use of the Nevis synchrocyclotron for neutron time-of-flight spectroscopy has been described previously in *Review of Scientific Instruments* papers in 1960[7] and 1964.[8] Reference should be made particularly to the 1964 description, since most of that over-all picture still applies. In the following description, we shall summarize the system, emphasizing the new features of the 1968 run.

The synchrocyclotron was operated at 70 bursts/sec of ~350-MeV protons, ~1.6 μA time-average current, on a Pb target for "evaporation neutron" production. When the proton bunch reached ~68-in. radius (~350 MeV) a vertical electrostatic deflector was pulsed to ~100 keV between the plates, rf-phase-correlated, to give a single-turn deflection of ~1 A proton current over an interval ~20 nsec full width. The protons struck the 1-in.-high ×3×8-in. Pb target, which was on top of the $1\frac{3}{4}$-in.-thick×3-in.-high×8-in.-long Al walled box through which recirculating water flowed for cooling and moderator action (new). The proton bursts on the Pb, ~20 nsec full width, gave $\gtrsim 10^{19}$ evaporation neutrons/sec instantaneous intensity. Those neutrons which were moderated in the water and left the front box face aimed at the distant

detectors constituted the useful pulsed neutron flux.

The flight path was mainly in He to reduce air scattering losses. The "transmission-sample position" was just outside the main 10-ft-thick cyclotron shield, where the collimated beam aperture was 2-in.-high×8-in. for natural-element samples or $1\frac{1}{4}$ in. high×5 in. for separated isotopes. The net cyclotron intensity was increased ~4 times from earlier runs. The new smaller aperture for separated-isotope samples was very important in allowing us to use thicker samples for a given sample mass.

The fast-neutron and γ-ray burst from the Pb target was blocked by aiming the flight path only at the moderator, along a path just below a barrier of ~6-in. thickness of stainless steel and Pb which was positioned inside the cyclotron chamber to help block the "view" of the Pb target. The main 200-m detector for transmission measurements used a B^{10} slab ~1.5 in. thick along the beam path×12 in. high×48 in. wide, which was viewed by a bank of NaI detectors from below out of the direct beam, to detect the 480-keV γ rays following the $B^{10}(n, \alpha)Li^{7*}$ capture process. For the 200-m path, the net path Δl half spread at half maximum was ~3 or 4 cm, including a contribution from the moderation time spread for each final energy E which acts like a length smearing.

The cyclotron building has been extended to include the old 35-m station, so the self-indication station was moved to ~40 m for the 1968 run. A new improved detector was used for this station, designed as shown in Fig. 1. It has a central rectangular aperture $3\frac{3}{4}$ in. high×$9\frac{3}{4}$ in. wide×21 in.

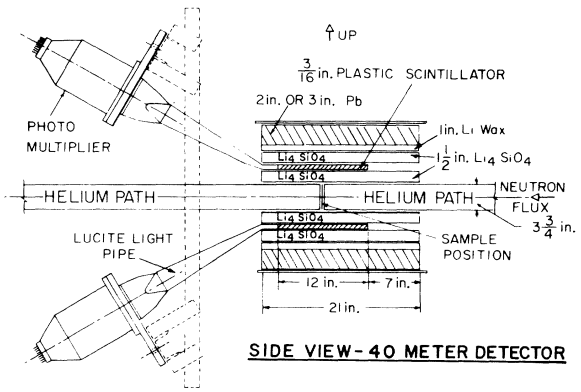

FIG. 1. The 39.57-m self-indication detector. The collimated neutron flux has a smaller area than the $3\frac{3}{4}$-in.-vertical by $9\frac{3}{4}$-in.-horizontal central aperture through the detector. The sample is positioned at midlength between He-filled boxes having thin Al end windows. Neutron-resonance capture γ rays from the sample produce recoil electrons in the Li_4SiO_4 converter which traverse the scintillator plastic.

long parallel to the flight path. The neutron flux, precollimated to miss the inside walls, could pass through and beyond, except for those interacting with the "*D* sample," which was positioned perpendicular to the beam at the center between He-filled front and back tubes. As shown in Fig. 1, the capture γ rays from the sample first traversed a $1\frac{1}{2}$-in.-thick layer of Li_4SiO_4, which served as a radiationless neutron-capture medium and as a γ-ray converter to produce secondary electrons as in a Moxon-Rae detector. The $\frac{3}{16}$-in.-thick scintillation plastic was in four parts (top, bottom, and sides), each viewed by its own photomultiplier via a light pipe. Another layer of Li_4SiO_4 came next, followed by 1 in. of LiF-impregnated wax and 2 or 3 in. of Pb shielding. The scintillation plastic was 12 in. long parallel to the flight path and subtended ~3π solid angle at the sample for good γ-detection efficiency. This new detector gave greatly reduced background-to-true-signal rates and was found to be only slightly sensitive to scattered neutrons when a carbon scatterer was introduced. As for a Moxon-Rae-type detector, the γ-detection efficiency showed no significant variation from level to level for a given target nucleus.

A main new feature was the use of an on-line EMR-type 6050 computer to replace the old, increasingly unreliable, 2000-channel-analyzer system.[8] The associated interface was built by the Pegram Labs electronics group under Dr. Jack Hahn. A 40-MHz free-running crystal oscillator had four output channels at 0, 90, 180, and 270° relative phase. The "start" pulse, which was random with respect to the oscillator, caused the best aligned phase output to subsequently feed the "clock" scaling circuit with only ±3-nsec maximum jitter relative to the start pulse. The 8192 histogram channels were divided into 16 groups of 512 channels. The channel widths could be adjusted separately for each group in powers of 2 times 25 nsec, and a variable delay could be used for the start of the first group. The 8192 channels were more than adequate for the 40-m detector, but not always sufficient for the 200-m detectors to cover simultaneously the full energy range of interest with appropriate energy resolution. Previously, with only 2000 channels, several separate runs using overlapping energy intervals were required to cover the full energy region of interest. Everything considered, the 1968 operation was many times as effective as any previous operating period.

The interface system with the "clock" had an associated fast (80-nsec) 6-word buffer derandomizer which fed count channel information to a larger (100–200-word) intermediate-speed (1.9-μsec/word) buffer, with later slower transfer to the main histogram storage each cyclotron cycle.

This permitted over 100 counts/burst to be collected. The $t=0$ position was determined by the (channel) position of the prompt-γ flash which had $\frac{2}{3}$-μsec transit time for 200 m. Each data counting period lasted ~30 to 60 min. The developing data histogram could be studied using a computer-associated oscilloscope display. Data were transferred to magnetic tape, and an Alden recording[8] was made for a permanent visual record and for study in planning subsequent measurements.

The detection channel widths were increased (in blocks of 512 channels) as the time of flight t increased such that $\Delta E/E$ due to the $\Delta t/t$ contribution was typically (200 m) 0.1% at 25 keV, 0.07% at 10 keV, 0.05% at 1 keV, and 0.1% at 50 eV, with a low-energy limit ~20 eV. For the 40-m detector it was 0.2% at 3 keV, 0.1% at 1 keV, and $\lesssim$0.1% at lower energies, with $\lesssim$1 eV as the lowest energy. The value of $\Delta E/E$ due to $\Delta l/l$ was ~0.04% at 200 m and 0.2% at 40 m, with the $\Delta l/l$ and $\Delta t/t$ contributions adding in quadrature.

III. PRELIMINARY DATA PROCESSING

During data collection we also used a monitor detector, which viewed the moderator via another collimated hole, to help correct for cyclotron-intensity changes. "Fast cycling" was also used to help obtain proper relative normalizations.[8] The proper data analysis was still quite complicated and, as mentioned earlier, required ~1 yr of intensive study of the systematics of the data before the data were properly reduced to a (T, σ) (transmission, cross section) format for subsequent resonance-parameter analysis. For the flat detector transmission measurements, the situation was far from the textbook situation because the neutron detectors were basically γ-ray detectors and thus subject to a quite significant dependence on the γ and n filtering by the sample and on the time after the burst. If not properly carried out, this part of the processing could lead to quite wrong Γ_n values and inconsistency between the Γ_n values implied for each level by the data from different sample thickness, etc.

Over the energy region of interest for the Er analysis (<10 keV) this analysis showed that the background (for equal Δt intervals) was always of an $A+BE^{\alpha}$ form, where A and B were sample-dependent constants and $\alpha \approx 0.6$. The evaluation of the A and B values was carried out by making use of favorable levels, where "bottoming dips" ($T=0$) occurred in the thick and medium-thick samples. After the background correction was made for these thicker samples, the ratio of the true count rate at the regions between levels for the thick sample to that for the medium sample gave T for the difference thickness, σ between levels, the implied background-corrected "open" count rate and the T values for other thicknesses of the same sample material. The excess actual thin-sample count rate was then equal to its background so the parameters A and B for the thin samples and "open" count rate could be obtained. It was required that the final set be self-consistent over the full energy interval. This could not be achieved unless the background corrections had been made correctly. Considerable care was taken to assure that this crucial processing was done properly.

IV. CONDITIONS FOR THE ERBIUM MEASUREMENTS

Natural erbium, $Z=68$, has atomic isotopic abundances and spin values (0.140%, 0) for 162; (1.58%, 0) for 164; (33.8%, 0) for 166; (22.9%, $\frac{7}{2}$) for 167; (27.0%, 0) for 168; and (14.7%, 0) for 170. All samples were of the form Er_2O_3. In addition to natural erbium samples, we had separated-isotope samples enriched, respectively, in Er^{166}, Er^{167}, Er^{168}, and Er^{170}. These materials were obtained on loan from the Isotope Division at Oak

TABLE I. Parameters for the separated-erbium-isotope samples. The samples were in the form Er_2O_3.

Main Isotope	Wt. of Er (g)	$1/n$ of Er	$1/n$ of isotopes Er^{166}	Er^{167}	Er^{168}	Er^{170}
Er^{166}	108.2	103	108.3	2750	8960	43 800
Er^{166}	73.3	152	160	4060	13 200	64 700
Er^{166}	34.9	319	336	8520	27 800	136 000
Er^{166}	17.5	637	672	17 100	55 600	272 000
Er^{167}	96.8	115	1980	132.4	1810	22 200
Er^{167}	79.3	141	2410	161.6	2210	27 100
Er^{167}	17.5	639	10 900	733	10 000	123 000
Er^{167}	8.75	1280	21 900	1470	20 000	245 000
Er^{168}	84.5	133	7560	4550	140.8	17 700
Er^{170}	105.9	107	10 100	10 900	5500	111.8

Ridge National Laboratory (ORNL). Various thickness samples of each separated isotope were prepared in the form of pressed slabs $1\frac{1}{4}$ in. × 5 in. A small amount of dilute polystyrene cement was used as a binder, and the samples were wrapped in thin Al foil for protection. Table I shows the parameters for the samples which were studied. Values of $1/n$ in b/atom are shown for the element and for each isotope. The main isotope has the *lowest* $1/n$ in each case. The abundances of Er^{164} and Er^{162} in these samples were listed as <0.1 and <0.05%, respectively. No resonances due to Er^{162} and Er^{164} were observed using the separated-isotope samples of Table I. Earlier transmission data had been obtained in 1965 using the 200-m detectors, $E \geq 56$ eV, for a separated-isotope sample of Er^{164} having $1/n = 4323$ (for Er^{164}). This was supplemented by the Brookhaven National Laboratory studies[9] using separated-Er-isotope samples with their reactor fast-chopper time-of-flight system. Their resolution was very much poorer than ours, but their transmission aperture was much smaller so they could use much thicker samples for a given sample mass. Their results for Er^{162} and Er^{164} are much more complete than ours in the low-energy region.

We also have 200-m transmission measurement data using larger-area format samples of natural

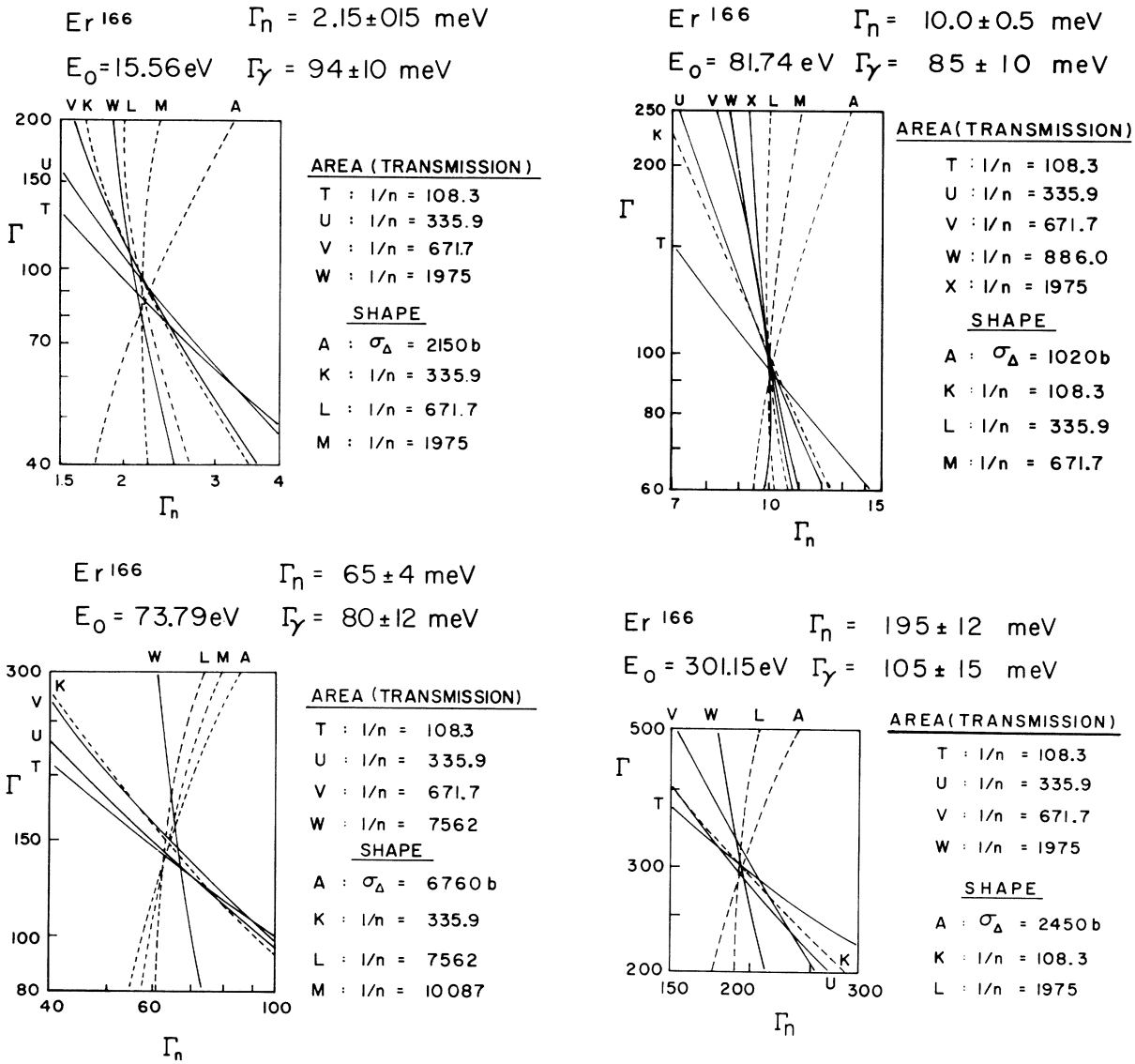

FIG. 2. Examples of resonance-parameter analysis for four levels of Er^{166}. The sample $1/n$ values are indicated for each curve.

Er_2O_3 with $1/n$ values of 15.0, 61.5, 149.7, and 298.6 for Er. The thickest sample permitted evaluation of between-level natural Er cross sections, and helped in obtaining better parameters for weak levels which had been identified from the separated-isotope data.

V. RESONANCE-PARAMETER EVALUATION

In the analysis of the data where resonance transmission dips are seen in flat detector transmission, or resonance peaks are seen in the D or $D+T$ self-indication (40-m) data, we do not attempt to determine the true σ vs E behavior directly. Since σ varies through many orders of magnitude at resonance and includes Doppler broadening, such a procedure would give very misleading results at resonance and the samples are too thin to evaluate the isotopic σ between levels. Rather, we use an inverse process and search for resonance parameters E_0, Γ_n, Γ which, when Doppler broadening of σ and instrumental broadening of the transmission T are considered, best *predict* the observed features. The implied true σ vs E can then be reconstructed if desired. The techniques where the area A under a transmission dip is used have been described in earlier papers.[1] The computer technology of carrying out the calculations has been greatly improved with time, but the basic ideas are the same. We have also made partial use of shape analysis (new) for favorable low-energy resonance data, where energy-resolution effects are small

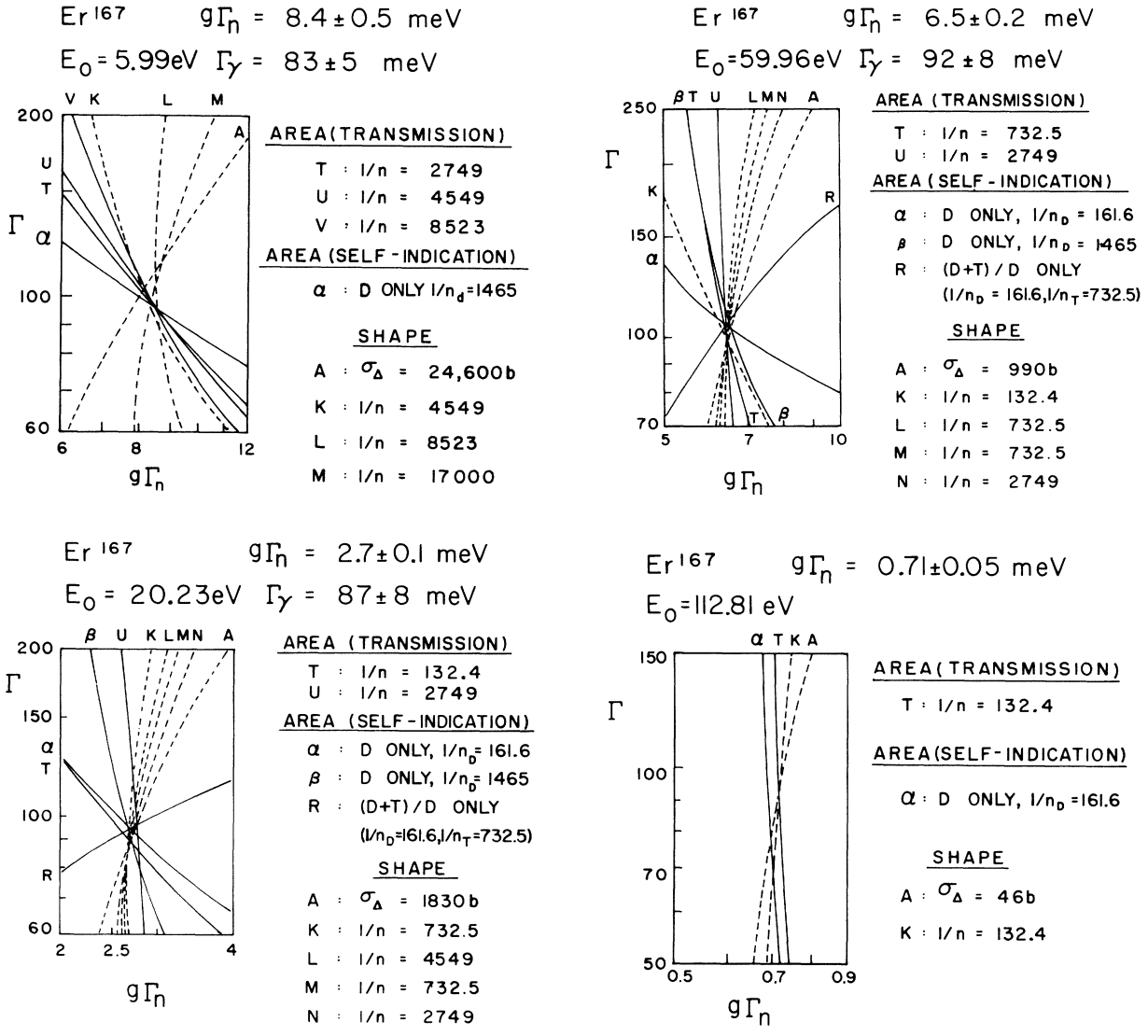

FIG. 3. Examples of resonance-parameter analysis for four levels of Er^{167}.

and the resonance is spread over a quite large number of channels. This might, for example, be a use of the sides of a bottoming resonance where T has a gradual recovery from zero. By doing this for different sample-thickness data for a given resonance, one establishes sets of $E_0+\Delta_1 E$ and $E_0-\Delta_2 E$ at which the Doppler-broadened resonance cross section has recovered to σ_1 and σ_2 values near the $1/n$ values for the samples. If the observed $T(E)$ has little curvature for a few channels on either side of the chosen points, this assures that resolution effects are not significant.

We can similarly make use of results for the peak cross section where the observed transmission dip $T_{\min}$ is not too low and is spread over several channels. Small corrections can be made for the experimental resolution from the curvature of observed T near $T_{\min}$. This can be done both for weak and strong low-energy resonances, since, for example, a strong resonance in Er^{166} will appear as a weak "impurity" resonance in the Er^{167} or Er^{168} data, where, however, the Er^{166} content is accurately known.

The analysis of the D-only and $D+T$ 40-m data is complicated by multiple-interaction phenomena which do not affect the transmission data. In transmission, *any* interaction will remove the neutron from the beam. In self-indication the observed process is resonance capture in the D sample which may be the first interaction to occur, or which may be preceded by 1, 2, ... prior energy-shifting scatterings in the sample. This multiple-interaction distortion is a well-known and annoying problem for experimenters who try to measure resonance capture or scattering directly. The effect is small on the low-energy side of resonance, since energy shifts are away from resonance and there is destructive interference between poten-

TABLE II. Resonance parameters of Er^{166} (also, see Table IX).

E_0 (eV)	ΔE_0	Γ_n^0 (meV)	$\Delta\Gamma_n^0$	E_0 (eV)	ΔE_0	Γ_n^0 (meV)	$\Delta\Gamma_n^0$	E_0 (eV)	ΔE_0	Γ_n^0 (meV)	$\Delta\Gamma_n^0$	E_0 (eV)	ΔE_0	Γ_n^0 (meV)	$\Delta\Gamma_n^0$
15.56	0.04	0.55	0.04	1757.8	0.5	4.7	0.5	3378.7	1.3	15	2	5845.7	3.1	29	5
73.79	0.07	7.6	0.5	1785.7	0.6	8.5	1.1	3415.4	1.3	10.3	1.2	5944.8	3.2	5.6	1.4
81.74	0.08	1.11	0.06	1809.6	0.6	3.8	0.6	3468.6	1.4	0.58	0.43	6022.4	3.2	6.2	1.8
110.63	0.08	0.006	0.003	1831.9	0.6	2.4	0.4	3519.4	1.4	17.4	2.4	6111.4	3.3	14	2.3
154.15	0.21	0.56	0.03	1846.4	0.6	14.5	1.6	3541.0	1.5	12.5	1.9	6274.8	3.3	7.8	1.5
170.98	0.25	34	2.3	1906.5	2.9	0.23	0.16	3600.9	1.5	4.3	0.8	6303.8	3.4	8.1	1.5
243.59	0.21	1.7	0.13	1940.2	0.6	3.8	0.45	3615.9	1.5	3.7	0.8	6348.5	3.5	8.4	1.5
301.15	0.29	11.2	0.7	1987.7	0.6	1.2	0.2	3630.6	1.5	2.0	0.5	6428.9	3.5	9.1	1.6
315.70	0.31	20	1	2027.5	0.7	0.73	0.16	3663.8	1.5	0.41	0.41	6475.0	3.6	5.8	0.9
352.23	0.36	4.9	0.4	2069.0	3.3	0.18	0.10	3755.0	1.6	13	1.6	6543.3	3.6	30	7.4
388.46	0.42	9.4	0.8	2121.6	0.7	9.9	1.5	3790.7	1.6	2.0	0.5	6556.0	3.6	25	6
457.88	0.19	0.07	0.05	2128.9	0.7	16	2.2	3841.5	1.6	13	2	6601.7	3.7	4.6	2.2
509.04	0.32	2.4	0.22	2174.5	0.7	4.7	0.54	3851.3	1.6	22	3.6	6701.9	3.8	9.2	2.4
535.32	0.34	2.3	0.22	2197.5	0.7	4.8	0.75	3895.0	1.6	6.1	1.1	6770.5	3.8	11	2.2
594.84	0.40	29	3	2245.4	0.7	8.1	1.0	3919.3	1.7	0.5	0.5	6870.7	3.9	2.2	2.2
601.01	1.03	0.17	0.10	2269.5	0.7	5	0.7	3982.1	1.7	11.6	1.6	7017.2	4.0	7.3	2.0
642.17	0.45	1.8	0.24	2364.5	0.8	1.2	0.2	4015.9	1.7	0.85	0.51	7057.6	4.1	1.8	0.7
708.29	1.32	0.105	0.045	2401.4	0.8	15	1.8	4047.4	1.8	0.82	0.50	7193.5	4.2	2	0.8
747.32	0.56	3.1	0.4	2463.2	0.9	1.8	0.3	4110.9	1.8	1.5	0.6	7222.8	4.2	7.3	1.8
772.84	0.59	1.4	0.2	2476.2	0.9	14	1.6	4152.7	1.8	6.7	1.1	7273.5	4.3	3.8	1.1
794.46	0.61	4.1	0.43	2514.0	0.9	7.3	1.0	4169.3	1.9	7.4	1.1	7354.8	4.3	18	3.5
848.95	0.34	33	2.4	2548.5	4.5	0.24	0.16	4233.5	1.9	4.3	0.7	7385.1	4.4	21	4
873.07	0.91	0.22	0.08	2569.0	0.9	19.5	2.2	4306.1	1.9	7.4	1.0	7477.2	4.4	10.6	1.9
905.02	0.37	16	1.7	2594.9	0.9	1.45	0.30	4349.0	2.0	7.4	1.0	7593.6	4.5	18	3
923.90	0.99	0.08	0.04	2656.4	0.9	23	2	4422.5	2.0	3.5	1.2	7636.8	4.6	4.6	1.6
973.94	1.06	0.08	0.04	2669.6	4.9	0.10	0.07	4488.7	2.1	1.0	0.5	7705.8	4.6	9.1	2.9
1025.1	0.5	7.8	0.8	2736.0	1.0	17.4	1.7	4616.9	2.1	1.4	0.9	7829.9	4.7	4.6	1.9
1036.9	1.2	0.25	0.10	2785.5	1.0	16.5	1.9	4652.6	2.2	6.5	1.0	7969.3	4.9	13.4	3.1
1056.8	0.5	4.8	0.5	2808.2	1.1	0.8	0.2	4688.6	2.2	1.5	0.7	8013.3	4.9	15.6	3.6
1137.2	0.5	2.4	0.3	2829.6	1.1	30	5	4759.7	2.3	0.96	0.51	8132.4	5.0	30	5
1171.0	0.5	8.9	0.7	2850.2	1.1	0.56	0.23	4857.9	2.3	5.2	1.2	8285.1	5.2	16	3.3
1183.7	0.5	16	1	2890.1	1.1	10	1.2	4902.2	2.4	21	4	8399.8	5.3	21	3.8
1259.5	0.6	4.9	0.45	2931.8	1.1	4.8	0.74	4936.4	2.4	19	3	8458.1	5.3	47	7.6
1325.0	1.7	0.13	0.09	2950.3	1.1	0.66	0.33	4985.4	2.4	21	3.4	8680.7	5.5	32	6.4
1339.7	0.6	1.8	0.22	2984.5	1.1	3.1	0.5	5036.4	2.5	2.8	1.0	8835.0	5.7	61	8.5
1367.3	0.7	27	2	3022.7	1.2	0.44	0.44	5140.8	2.5	5.2	1.1	9016.7	5.9	4.1	2.1
1431.3	1.9	0.2	0.13	3040.9	1.2	1.1	0.7	5314.4	2.6	12.6	2.1	9075.6	5.9	16	4
1468.6	0.8	2.4	0.3	3068.5	1.2	0.47	0.47	5416.6	2.7	8.8	1.6	9195.1	6.1	26	5
1502.3	0.8	16.5	1.3	3127.3	1.2	0.54	0.39	5449.5	2.7	1.5	0.8	9274.8	6.2	4.4	1.9
1545.6	2.1	0.07	0.05	3147.0	1.2	3.3	0.5	5561.3	2.8	6.8	1.1	9373.4	6.2	8	3
1556.2	0.9	7.4	0.7	3214.9	1.2	7.7	0.9	5609.9	2.9	5.3	0.9	9429.6	6.2	17	3.6
1618.1	2.3	0.17	0.09	3280.7	1.3	6.5	0.8	5729.6	3.0	16	2.6	9486.2	6.3	22	5
1640.5	0.9	3.5	0.5	3340.8	1.3	6.9	1.1	5780.4	3.0	2.1	0.9				
1678.9	2.4	0.09	0.06	3351.4	1.3	10.5	1.6	5800.0	3.0	19	3.4				

TABLE III. Resonance parameters of Er^{167} (also, see Table X).

E_0 (eV)	ΔE_0	Γ_n^0 (meV)	$\Delta\Gamma_n^0$
0.460[a]		0.46	0.04
0.584[a]		0.32	0.03
5.99	0.02	6.9	0.4
7.92	0.03	0.078	0.008
9.39	0.03	2.2	0.14
20.23	0.05	1.20	0.04
22.02	0.06	0.24	0.012
26.24	0.15	15.6	1.2
27.42	0.08	2.3	0.16
32.88	0.04	1.33	0.07
37.59	0.05	1.30	0.07
39.43	0.06	1.37	0.07
42.23	0.06	0.55	0.03
50.19	0.08	1.10	0.06
53.60	0.09	8.7	0.8
59.96	0.05	1.68	0.05
62.07	0.05	0.81	0.05
62.78	0.06	0.78	0.05
69.43	0.06	0.31	0.03
74.37	0.07	0.69	0.09
75.77	0.07	0.13	0.01
79.29	0.08	1.01	0.11
85.42	0.09	0.134	0.012
91.22	0.10	0.36	0.022
94.80	0.10	1.97	0.23
97.57	0.11	0.098	0.010
98.20	0.14	0.024	0.016
107.57	0.12	4.4	0.2
112.81	0.13	0.13	0.01
115.55	0.14	0.30	0.02
128.27	0.21	0.034	0.014
131.56	0.17	8.5	0.44
142.12	0.19	1.34	0.09
142.86	0.19	0.15	0.026
150.45	0.20	0.158	0.014
153.18	0.27	0.048	0.020
157.78	0.22	4.5	0.32
159.42	0.22	0.51	0.064
162.21	0.23	2.2	0.16
165.08	0.23	1.56	0.16
166.83	0.24	3.6	0.38
168.49	0.24	3.7	0.38
176.76	0.13	0.62	0.06
178.45	0.13	2.5	0.16
184.74	0.14	1.25	0.074
191.31	0.15	1.97	0.15
195.95	0.15	5.3	0.28
209.87	0.17	2.7	0.22
217.22	0.18	0.66	0.054
223.30	0.18	0.23	0.04
228.69	0.19	3.2	0.26
230.03	0.19	0.28	0.066
235.47	0.20	1.50	0.13
237.86	0.20	1.76	0.13
238.67	0.20	0.56	0.13
247.27	0.21	0.69	0.09
249.09	0.22	1.13	0.13
258.18	0.23	4.5	0.4
263.25	0.24	1.54	0.16
274.47	0.25	1.45	0.12
279.91	0.26	4.8	0.6
282.49	0.26	7.6	0.9
288.83	0.27	0.54	0.08
297.56	0.30	0.128	0.034
304.69	0.38	0.046	0.034
306.18	0.30	0.138	0.034
309.50	0.30	1.53	0.16
314.20	0.31	0.37	0.11
319.44	0.31	2.20	0.22
327.22	0.32	1.33	0.13
329.95	0.33	0.28	0.09
331.64	0.33	4.8	0.56
335.14	0.34	3.7	0.32
343.00	0.35	4.1	0.32
346.50	0.36	2.3	0.22
349.71	0.36	3.4	0.32
355.51	0.37	0.35	0.06
358.09	0.37	0.22	0.05
363.72	0.38	5.2	0.32
368.32	0.39	1.83	0.17
371.04	0.39	0.20	0.04
373.40	0.40	0.35	0.06
376.58	0.40	0.57	0.08
381.84	0.41	1.4	0.18
384.30	0.41	0.26	0.06
387.62	0.42	5.0	0.4
393.54	0.43	0.10	0.05
396.55	0.43	0.13	0.05
399.59	0.43	2.7	0.26
408.04	0.45	0.82	0.12
411.67	0.46	0.58	0.10
414.63	0.59	0.07	0.04
418.76	0.24	0.14	0.04
422.66	0.24	1.5	0.2
429.04	0.24	1.7	0.2
433.94	0.25	0.33	0.13
437.18	0.25	3.4	0.4
440.45	0.25	0.32	0.11
442.23	0.25	0.29	0.10
446.59	0.26	4.2	0.42
455.77	0.27	1.73	0.14
461.96	0.27	0.39	0.07
466.61	0.28	2.4	0.23
473.59	0.28	4.3	0.36
450.43	0.29	5.2	0.54
485.37	0.29	5.1	0.54
497.30	0.30	7.4	1.4
498.82	0.30	4.0	0.8
505.91	0.31	2.8	0.44
508.10	0.32	2.0	0.36
515.38	0.32	0.48	0.09
518.93	0.32	0.37	0.09
522.17	0.33	0.19	0.11
528.27	0.33	9.3	1.8
531.45	0.34	0.57	0.14
533.13	0.34	0.31	0.09
542.34	0.35	3.2	0.26
550.03	0.35	1.19	0.17
555.01	0.36	0.85	0.26
556.80	0.36	3.5	0.5
562.60	0.37	1.77	0.25
571.52	0.37	5.2	0.84
575.47	0.38	2.6	0.42
580.99	0.39	0.30	0.15
590.10	0.39	5.8	0.66
612.71	0.42	3.4	0.32
629.88	0.44	0.69	0.15
636.86	0.44	4.1	0.4
648.45	0.45	0.33	0.14
652.54	0.46	4.2	0.48
665.98	0.47	1.63	0.23
675.97	0.48	1.38	0.23
677.90	0.48	2.1	0.3
691.63	0.50	0.65	0.15
693.13	0.50	0.76	0.19
708.88	0.52	2.0	0.23
711.99	0.52	0.37	0.15
723.04	0.53	1.41	0.23
726.24	0.53	1.0	0.19
729.47	0.54	4.1	0.52
737.08	0.55	1.03	0.29
741.48	0.55	1.54	0.22
750.40	0.56	0.47	0.24
753.23	0.57	1.24	0.29
757.20	0.57	0.69	0.15
772.84	0.59	5.8	1.5
776.36	0.60	13.3	2.2
784.74	0.60	0.42	0.14
790.79	0.61	2.5	0.4
800.01	0.62	2.1	0.36
803.11	0.62	0.51	0.14
808.12	0.63	2.4	0.36
811.21	0.64	0.21	0.07
816.36	0.64	2.6	0.36
820.92	0.32	3.0	0.4
823.91	0.32	0.28	0.07
838.24	0.33	2.8	0.28
852.35	0.34	1.09	0.34
855.07	0.34	2.6	0.34
865.07	0.35	3.0	0.4
883.45	0.36	1.35	0.20
886.61	0.37	0.64	0.20
888.59	0.37	1.48	0.34
896.15	0.37	10.4	1.1
914.02	0.38	5.4	0.66
918.57	0.38	2.0	0.34
930.09	0.39	1.58	0.20
935.75	0.39	4.1	0.72
939.47	0.40	3.7	0.66
944.61	0.40	0.59	0.18
950.59	0.40	1.49	0.33
956.23	0.40	0.78	0.13
958.96	0.41	0.17	0.10
961.81	0.41	0.97	0.32
966.00	0.41	0.51	0.16
968.47	0.41	0.48	0.13
972.60	0.42	2.4	0.26
984.32	0.42	7.1	0.9
991.54	0.43	0.44	0.13
995.82	0.43	0.61	0.22
998.83	0.43	6.1	0.88
1014.0	0.4	2.9	0.38
1018.4	0.5	0.81	0.25
1022.0	0.5	13.1	2.5
1035.5	0.5	0.90	0.22
1047.5	0.5	1.08	0.25
1065.8	0.5	0.37	0.18
1068.9	0.5	1.53	0.37
1073.9	0.5	3.7	0.56
1091.0	0.5	0.85	0.36
1101.4	0.5	1.11	0.27
1108.4	0.5	1.56	0.36
1115.0	0.5	2.2	0.42
1123.7	0.5	3.0	0.48
1129.9	0.5	0.34	0.17
1138.8	0.5	0.77	0.36
1144.1	0.5	1.24	0.30
1159.0	0.6	1.68	0.41
1163.9	0.6	0.46	0.23
1166.1	0.6	0.55	0.27
1173.7	0.6	0.49	0.21
1193.2	0.6	0.98	0.18
1201.1	0.6	0.70	0.15
1206.8	0.6	5.5	0.7
1219.5	0.6	2.6	0.6
1223.6	0.6	1.9	0.52
1226.6	0.6	7.1	1.4
1230.1	0.6	0.41	0.21
1234.2	0.6	0.43	0.22
1237.8	0.6	0.57	0.12
1243.8	0.6	0.49	0.25
1248.3	0.6	0.52	0.17
1252.2	0.6	1.58	0.40
1254.6	0.6	1.75	0.45
1265.6	0.6	0.56	0.11
1269.3	0.7	2.8	0.46
1273.7	0.7	1.29	0.34
1279.9	0.7	3.9	0.96
1284.5	0.7	15.6	2.6
1289.2	0.7	1.0	0.45
1293.0	0.7	0.95	0.45
1299.4	0.7	0.44	0.22
1303.9	0.7	3.1	0.61
1314.9	0.7	1.65	0.50
1318.8	0.7	0.83	0.33
1324.1	0.7	0.71	0.33
1326.7	0.7	2.0	0.44
1336.0	0.7	1.37	0.28
1350.8	0.7	3.8	0.76
1361.7	0.7	1.16	0.66
1372.1	0.7	0.86	0.33
1379.1	0.7	1.7	0.43
1388.2	0.7	8.6	1.7
1399.6	0.7	5.7	0.96
1407.5	0.7	0.64	0.32
1415.0	0.7	1.65	0.64
1419.7	0.8	1.54	0.53
1425.2	0.8	2.8	0.64
1432.6	0.8	1.69	0.42
1439.3	0.8	6.3	1.2
1442.8	0.8	0.50	0.27
1456.4	0.8	2.4	0.52
1462.9	0.8	1.41	0.53
1471.3	0.8	5.5	1.2
1482.0	0.8	1.9	0.57
1485.9	0.8	0.88	0.31
1493.6	0.8	1.04	0.52
1495.9	0.8	2.4	0.78
1507.9	0.8	1.8	0.57
1517.5	0.8	6.2	1.3
1524.0	0.8	3.1	0.76
1528.1	0.8	1.07	0.46
1538.8	0.8	6.9	1.0
1544.6	0.8	7.6	1.3
1552.9	0.8	8.6	1.5
1563.8	0.8	1.06	0.46
1568.5	0.9	6.1	1.4
1571.5	0.9	1.51	0.76
1581.7	0.9	1.21	0.40
1591.2	0.9	2.7	0.6
1607.0	0.9	1.25	0.30
1611.4	0.9	2.2	0.5
1622.1	0.9	2.1	0.6
1637.3	0.9	0.84	0.40
1641.9	0.9	6.4	1.7
1652.8	0.9	1.03	0.44
1658.8	0.9	15.0	2.4
1675.8	1.0	4.3	1.2
1680.0	0.5	5.4	1.5
1686.4	0.5	1.27	0.54

[a] Parameters for the resonances below 1 eV from H. B. Moller *et al.*, Nucl. Sci. Eng. 8, 183 (1960).

TABLE IV. s-wave resonance parameters of Er^{168} (also see Table IX). For the "selected" s population to 4.7 keV, we add "missed" s levels at 646 and 2045 eV as discussed in the text.

E_0 (eV)	ΔE_0	Γ_n^0 (meV)	$\Delta\Gamma_n^0$	E_0 (eV)	ΔE_0	Γ_n^0 (meV)	$\Delta\Gamma_n^0$	E_0 (eV)	ΔE_0	Γ_n^0 (meV)	$\Delta\Gamma_n^0$	E_0 (eV)	ΔE_0	Γ_n^0 (meV)	$\Delta\Gamma_n^0$
79.70	0.12	4.9	0.34	2682.7	1.0	44	6.8	5449.5	2.8	27	4.7	9392	6	9.2	4.7
188.94	0.14	5.8	0.3	2814.2	1.0	2.7	0.75	5463.3	2.8	5.0	1.9	9614	6	11.7	3.6
244.42	0.42	35	1.9	2862.6	5.4	0.60	0.26	5703.0	3.0	23	2.7	9731	7	24	5.6
312.63	0.31	9.9	0.7	2970.6	1.1	5.8	1.3	5756.5	3.0	42	4.6	9824	7	78	12
410.82	0.29	0.10	0.04	3095.3	1.2	11.7	1.5	5968.4	3.2	20	2.8	10093	7	10	2.5
445.96	0.33	0.11	0.04	3165.8	1.2	3.8	0.8	6080.4	3.3	7.4	2.6	10159	7	11.4	3.0
527.11	0.33	36	3	3304.1	1.3	52	6.1	6249.3	3.4	77	8.9	10272	7	17.3	5.4
765.25	0.58	2.8	0.33	3467.2	1.4	3.7	1.2	6428.9	3.5	7.2	1.9	10423	7	16.2	4.9
830.33	0.33	35	3.5	3588.4	1.5	3.7	0.92	6528.8	3.6	7.7	2.5	10789	8	96	16
1005.8	0.5	13	1	3648.7	1.5	2.8	0.75	6565.1	3.6	9.0	3.1	11167	8	34	7
1093.9	0.5	30	2.1	3678.3	1.6	66	8.2	6627.4	3.7	11.3	3.4	11232	8	44	9.4
1131.7	0.5	6.1	0.74	3751.6	4.0	0.47	0.26	6759.1	3.8	23	3.7	11497	9	43	6.5
1342.8	1.8	0.24	0.11	3809.9	1.6	5.5	1.1	6859.0	3.9	15.1	4.8	11807	9	13.8	6.4
1356.3	0.7	8.7	0.87	3997.7	1.7	1.74	0.55	7017.2	4.0	17.3	2.4	12048	9	18.2	7.3
1449.6	0.8	24	2	4098.3	1.8	45	4.7	7231.2	4.2	34	4.1	12533	10	21	8.9
1626.1	0.9	2.5	0.35	4154.6	1.8	61	5.6	7441.9	4.4	45	5.6	12846	10	31	7
1713.9	0.5	1.59	0.31	4284.3	4.9	0.93	0.49	7593.6	4.5	8.7	3.5	13150	11	15.7	7.0
1810.7	0.5	5.4	0.71	4326.5	1.9	24	2.4	7625.4	4.6	8.3	4.1	13351	6	8.1	4.0
1894.4	0.6	11.8	1.3	4389.5	2.0	25	3	7780.4	4.7	6.8	2.3	13614	6	10.3	4.3
1937.3	1.2	33	3.4	4515.6	2.1	6.5	1.2	8157.6	5.1	16.6	3.3	13862	6	11.5	3.4
2151.9	0.7	6.6	0.86	4643.6	5.6	0.72	0.38	8378.8	5.3	51	7.7	13963	6	127	25
2204.3	0.7	9.3	1.1	4671.1	2.2	10.8	1.5	8702.9	5.6	64	9.9	14082	6	26	6
2364.1	0.8	32	3.3	4819.9	5.9	0.32	0.15	8877.7	5.7	23	8.5	14163	6	27	6
2472.4	0.9	2.2	0.4	4885.8	2.3	22	2.4	8900.7	5.8	6.9	3.5	14337	6	22	6.3
2544.0	4.5	0.58	0.20	5138.2	2.5	10.5	1.4	9117.2	6.0	50	9.4	14497	6	16.6	4.2
2671.4	1.0	22	3.9	5326.4	2.7	10.6	1.4	9156.0	6.0	15.7	5.8	14605	6	72	15

tial and resonance scattering. It is correspondingly of increased importance above resonance. For the Er data for which self-indication data were used, corrections due to these effects were usually $\lesssim 20\%$ so correction programs which we have developed could be used with good accuracy for each trial set of parameters used in an "area" analysis of the "D-only" peaks. One can usually obtain an accurate evaluation of the channel for exact resonance from the thinnest D-only sample, or from a "$D+T$" curve using a thin T sample which gives a sharp inversion dip at exact resonance.

A partial shape analysis for the ratio of the peak of the $D+T$ curve to that of the D curve was used successfully for ~20 favorable levels.

The procedure in all cases is to calculate, for each of a set of trial values for Γ/Δ, a value for $ng\,\Gamma_n$ which best matches the area or shape feature to be fitted. Here Δ is the Doppler width, which is known[1] as a function of E_0 and the sample atomic weight A, while g is the spin statistical weight factor, which is unity for the even-even target nuclei. Each "fit" to one experimental parameter, such as an area of a resonance dip, yields a curve of implied Γ_n vs test Γ. A thick-sample area tends to yield a quantity proportional to $\sigma_0\Gamma^2$, or $\Gamma_n\Gamma$. A thin-sample area may be proportional to $\sigma_0\Gamma$, or to Γ_n alone. An evaluation which emphasizes σ_0 (the peak cross section) tends to give Γ_n/Γ. The results for different sample-thickness transmission for self-indication and for partial shape analysis then each give curves of implied Γ_n vs Γ which, when all is well, intersect with varying crossing slopes about a "best-choice" locus (Γ_n, Γ) for that resonance.

TABLE V. p-wave resonance parameters of Er^{168}.

E_0 (eV)	ΔE_0	$g\,\Gamma_n$ (meV)	$\Delta g\,\Gamma_n$	$g\,\Gamma_n^1$ (meV)	$\Delta g\,\Gamma_n^1$	E_0 (eV)	ΔE_0	$g\,\Gamma_n$ (meV)	$\Delta g\,\Gamma_n$	$g\,\Gamma_n^1$ (meV)	$\Delta g\,\Gamma_n^1$
139.58	0.12	0.11	0.04	23	8	1207.7	1.5	2.6	1.6	22	13
145.71	0.12	0.06	0.05	12	10	1636.4	2.3	4.4	2.4	23	13
174.29	0.16	0.15	0.07	23	11	1681.3	2.4	3.0	2.4	15	12
296.67	0.36	0.29	0.16	20	11	2100.6	3.4	8.2	4.1	30	15
335.47	0.43	0.85	0.55	48	31	2325.9	3.9	4.3	3.4	13	11
587.43	0.50	0.49	0.40	12	10	2456.6	4.3	5.3	4.0	15	12
691.46	0.64	1.0	0.6	19	12	2900.5	5.5	21	12	47	27
985.73	1.08	2.0	1.2	23	14	3027.4	5.8	14	9	29	19
990.61	1.09	2.5	1.4	28	16	3202.8	6.3	8.5	5.0	16	10
1022.4	1.2	1.7	1.2	18	13	3849.9	4.2	14	8	21	12
1106.1	1.3	3.9	2.0	37	19	4127.0	4.7	13	10	17	14
1193.2	1.5	2.2	1.5	19	13	4476.8	5.3	14	10	16	12

TABLE VI. s-wave resonance parameters of Er^{170}.

E_0 (eV)	ΔE_0	Γ_n^0 (meV)	$\Delta\Gamma_n^0$	E_0 (eV)	ΔE_0	Γ_n^0 (meV)	$\Delta\Gamma_n^0$	E_0 (eV)	ΔE_0	Γ_n^0 (meV)	$\Delta\Gamma_n^0$	E_0 (eV)	ΔE_0	Γ_n^0 (meV)	$\Delta\Gamma_n^0$
95.07	0.10	90	4	3843.9	1.7	4.8	1.1	10229	7	40	6	17012	8	35	8.4
284.03	0.26	34	2.1	4123.6	1.8	5.6	0.8	10329	7	82	12	17058	8	34	8.4
496.69	0.30	30	1.8	4193.3	1.9	18.2	1.9	11103	8	7.7	2.9	17320	8	45	9.9
598.18	0.51	0.17	0.06	4240.9	1.9	21	2.2	11208	8	73	13	17773	8	58	11
748.72	0.56	4.6	0.55	4421.5	2.0	22	2.3	11281	8	17.9	5.7	18492	9	22	6.6
935.55	0.39	52	3.3	4599.6	5.5	1.6	0.7	11480	8	85	13	18621	9	106	16
975.00	1.06	0.26	0.09	4715.1	2.2	20	2	11557	9	7.2	3.6	19319	9	35	6.5
1089.0	0.5	23	1.5	5449.5	2.8	66	6.8	11608	9	47	7.4	19536	10	43	11
1230.7	0.6	1.08	0.20	5946.4	3.2	153	26	11702	9	19	9.2	19978	10	38	7.8
1391.1	0.7	76	5.4	6032.0	3.2	31	3.9	11798	9	14.7	5.5	20301	10	19.7	4.9
1524.0	0.8	1.82	0.41	6235.8	3.4	61	6.3	12428	9	77	11	20566	10	119	21
1844.1	2.8	0.58	0.26	6385.0	3.5	3.9	1.5	13212	9	46	8.7	21003	10	53	11
2009.6	0.6	24	1.8	6638.5	3.7	14.1	2.7	13465	5	8.6	3.0	21102	11	96	18
2101.1	0.7	31	2.2	6831.9	3.9	5.1	2.4	13806	6	50	8	21517	11	45	8.2
2190.9	3.6	1.13	0.43	6862.9	3.9	9.2	3.4	13932	6	70	10	21939	11	115	20
2249.3	0.7	45	3.4	7187.2	4.2	7.6	1.2	14569	6	29	5	22322	12	27	10
2377.9	0.8	11.7	1.6	7286.2	4.3	36	5	15404	7	10.9	3.2	22374	12	31	11
2594.0	4.6	0.75	0.32	8223.5	5.1	14.3	2.7	15609	7	80	13	22587	12	65	12
2830.6	1.0	84	8.5	8311.0	5.2	71	11	15777	7	49	7.2	22803	12	25	8.6
2977.8	1.1	3.3	0.46	8405.1	5.3	260	38	16045	7	54	8.7	22904	12	28	11
3302.1	1.3	11.3	1.2	8894.9	5.8	13.3	3.2	16142	7	87	16	23240	12	82	20
3352.8	3.4	0.95	0.42	9348.6	6.2	17.6	5.2	16448	7	41	8.6	23695	12	55	13
3464.4	1.4	3.3	1.2	9803.8	6.6	63	7.6	16488	8	13.6	4.7				
3715.9	1.6	1.92	0.66	10054	7	15	4.5	16869	8	73	14				

Examples of this are shown in Figs. 2(a)–2(d) for Er^{166}, and 3(a)–3(d) for Er^{167}. Only transmission measurements were used for other than very weak levels of the even Er isotopes. Plots such as those in Figs. 2 and 3 were prepared for *every* resonance for which parameter results are given. The labels on the figures should be self-explanatory as to the experimental quantity being fitted for each curve on each figure. Note that the thickest-sample area always results in one extreme curve which has ~45° downward slope from left to right, while the σ_Δ shape analysis (σ_Δ is the Doppler-broadened peak cross section) has a quite different slope which goes upward from left to right.

The "D-only" analysis makes use of the concept of an "absolute saturation" rate S_A as described in our earlier papers,[1] I and II. This S_A is the rate which would hold if *all* neutrons were captured by the isotope. The evaluated S_A curves all follow a common $E^{0.6}dt$ fit, which suggests that there is no serious dependence of the capture sensitivity on the γ-cascade pathway ratios from resonance to resonance. This is also shown by the consistency of the D-only level analysis with that using flat detector transmission measurements.

In actual practice, the analysis curve most different from that for thick-sample transmission is obtained from the ratio of the "$D+T$" peak area to that for D only, without using the experimental "wing-area" contribution, but by using wing corrections based on the assumed level parameters.

The results of these analyses constitute the foundation for this paper and the subsequent tests of fits to statistical theories. Tables II–VII present the level parameters for Er^{166}, Er^{167}, Er^{168}, and Er^{170}. For Er^{168} and Er^{170}, those levels which con-

TABLE VII. p-wave resonance parameters of Er^{170}.

E_0 (eV)	ΔE_0	$g\Gamma_n$ (meV)	$\Delta g\Gamma_n$	$g\Gamma_n^1$ (meV)	$\Delta g\Gamma_n^1$	E_0 (eV)	ΔE_0	$g\Gamma_n$ (meV)	$\Delta g\Gamma_n$	$g\Gamma_n^1$ (meV)	$\Delta g\Gamma_n^1$
164.59	0.15	0.066	0.045	11	8	1938.9	3.0	6.5	3.5	27	14
221.91	0.23	0.71	0.21	75	22	2087.2	3.4	3.7	3.0	14	11
394.31	0.28	0.54	0.25	24	11	2291.0	3.9	16	7	51	22
408.93	0.29	1.3	0.4	55	17	2482.3	4.3	14	7	40	20
483.76	0.37	0.95	0.50	31	16	2857.3	5.4	27	19	62	44
584.12	0.50	2.3	0.9	57	22	2928.0	5.6	9.5	6.0	21	13
698.18	0.65	1.8	0.8	34	15	3018.6	5.8	21	9	44	19
729.50	0.69	2.2	1.0	39	18	3083.4	6.0	20	8	41	17
809.18	0.81	0.97	0.60	15	9	3150.3	6.2	15	6	30	12
1433.2	1.9	2.9	2.1	19	14	3414.7	3.5	34	16	60	28
1512.1	2.1	8.5	4.5	50	27	3518.1	3.7	7.3	5.0	12.3	8.4
1618.1	2.3	3.4	2.2	18	12	3599.7	3.8	28	11	46	18
1693.4	2.4	5.8	3.0	29	15	3698.0	4.0	9.3	6.0	14.5	9.4
1827.6	2.7	12	6	54	27	4067.4	4.6	9	7	12.2	9.5
1874.9	2.9	12	5	52	22	4318.8	5.0	36	21	45	26

TABLE VIII. Resonance parameters of Er^{164}. Since the conditions for the Er^{164} measurement could have involved our missing many resonances, even when they are strong, we do not give statistical parameters such as S_0, $\langle D \rangle$, etc.

E_0 (eV)	ΔE_0	Γ_n^0 (meV)	$\Delta\Gamma_n^0$	E_0 (eV)	ΔE_0	Γ_n^0 (meV)	$\Delta\Gamma_n^0$	E_0 (eV)	ΔE_0	Γ_n^0 (meV)	$\Delta\Gamma_n^0$	E_0 (eV)	ΔE_0	Γ_n^0 (meV)	$\Delta\Gamma_n^0$
30.54	0.10	0.70	0.07	136.95	0.09	1.28	0.21	225.43	0.18	4.3	0.53	750.2	0.06	5.2	1.5
56.61	0.09	0.96	0.11	160.73	0.18	4.7	0.63	419.95	0.24	13	1.5				
108.59	0.06	4.1	0.6	194.63	0.14	4.9	0.65	611.57	0.24	7.0	1.4				
130.96	0.08	8.5	0.9	214.97	0.17	1.3	1.3	654.24	0.46	3.1	1.0				

stitute our selection for the s-level populations are listed first, with those considered most likely to be p levels given in the following tables. Since we have no specific tests for s vs p for levels, there may be errors in these assignments. The details for making the separations are given below. The $g\Gamma_n^1$ values are calculated using $g\Gamma_n^1 = \Gamma_n^0$ (350 keV/E), where the exact factor depends on our choice of nuclear radius[10] as $R = 1.4A^{1/3} \times 10^{-13}$ cm. When different S_1 values are given by different authors, one should note the assumed radius used in each case to convert Γ_n values to $g\Gamma_n^1$ values. The result is inversely proportional to R^2.

Results for our older data for Er^{164}, given in Table VIII, are of a much poorer quality, but are included for completeness. Tables IX and X list results for cases where Γ_γ and/or the compound nucleus J (for $n + Er^{167}$) have been evaluated.

VI. LEVEL SPACING SYSTEMATICS FOR THE ORTHOGONAL ENSEMBLE

The analysis of the systematics of our results tends to be dominated by the fact that the level spacing systematics are in good agreement with the statistical predictions for an orthogonal ensemble. A review of the pertinent theory, including the results of our extensive model calculations are, therefore, outlined before giving the detailed comparison of our results with theory. We are grateful to Professor Freeman Dyson for many discussions and valuable suggestions on this subject.

Before ~1956, there was no systematic statistical theory of level spacing ordering. An experimental relative shortage of small spacings tended to be dismissed as being due to instrumental resolution failings until Professor E. Wigner suggested his famous spacing law, Eq. (1). He indicated a belief that the levels for a single population should follow the same ordering behavior as do the eigenvalues for (large) real square $N \times N$ symmetric matrices with random Gaussian-distributed elements. The joint probability distribution is the "Wishart" distribution, which is proportional to the product of the absolute spacings $|E_k - E_j|$ for each level pair treated only once, times a Gaussian in $\sum_j E_j^2$ which prevents a spacing "blowup." This model is now called the Gaussian orthogonal ensemble (G.O.E.). Wigner showed that the eigenvalue distribution density is peaked at the middle and falls off according to a semicircle law on either side, except for a few levels in the extreme wings on either side. Since the intrinsic mean s-level density is essentially constant over the few keV regions of experimental comparison, one must either make $N \gg$ the number of levels and just use the center region where the density is essentially constant, or use a transformation to a new energy parameter for which the density is constant except in the omitted wings. A large number of theorists have studied this mathematical problem using both analytic and Monte Carlo methods. The papers, both published and unpublished to 1964 are collected in a book by Porter.[3] A later review is given by Mehta.[11] The nearest-neighbor spacing distribution was found by Gaudin[12] not to have exactly the Wigner form [Eq. (1)], but the difference was less than can be distinguished experimentally. Calculations were also made of the spacing distribution for levels having k levels between,[13] etc., which showed a short-range ordering for the levels beyond that expected for a set of uncorrelated adjacent Wigner [Eq. (1)] distributed spacings (U.W.).

TABLE IX. Parameters of the levels in Er^{166} and Er^{168} for which Γ_γ is obtained.

Er^{166}				Er^{166}				Er^{168}			
E_0 (eV)	ΔE_0	Γ_γ (meV)	$\Delta\Gamma_\gamma$	E_0 (eV)	ΔE_0	Γ_γ (meV)	$\Delta\Gamma_\gamma$	E_0 (eV)	ΔE_0	Γ_γ (meV)	$\Delta\Gamma_\gamma$
15.56	0.04	94	10	243.59	0.21	100	20	79.70	0.12	78	15
73.79	0.07	80	12	301.15	0.29	105	15	188.94	0.14	86	12
81.74	0.08	85	10	315.70	0.31	110	25	244.42	0.42	90	15
154.15	0.21	89	12	352.23	0.36	90	15	312.63	0.31	95	15
170.98	0.25	110	30	535.32	0.34	96	20				

TABLE X. Parameters of the levels in Er^{167} for which Γ_γ is obtained and J where determined.

E_0 (eV)	ΔE_0	Γ_γ (meV)	$\Delta\Gamma_\gamma$	J	E_0 (eV)	ΔE_0	Γ_γ (meV)	$\Delta\Gamma_\gamma$	J	E_0 (eV)	ΔE_0	Γ_γ (meV)	$\Delta\Gamma_\gamma$	J
5.99	0.02	83	5		166.83	0.24	84	15		349.71	0.36	92	20	
9.39	0.03	84	9		168.49	0.24	85	18		363.72	0.38	90	14	4
20.23	0.05	87	8		178.45	0.13	82	14		368.32	0.39	83	16	
22.02	0.06	87	12		184.74	0.14	90	15		387.62	0.42	82	10	3
26.24	0.15	90	15		191.31	0.15	98	20		399.59	0.43	82	12	4
27.42	0.08	83	14		195.95	0.15	90	9	4	429.04	0.24	66	20	
32.88	0.04	92	8		209.87	0.17	93	10	4	437.18	0.25	92	22	
37.59	0.05	82	8		228.69	0.19	102	20		446.59	0.26	90	20	
39.43	0.06	87	9		258.18	0.23	93	12	4	455.77	0.27	88	10	3
42.23	0.06	100	12		263.25	0.24	92	16		466.61	0.28	91	18	
50.19	0.08	82	10		279.91	0.26	92	20		473.59	0.28	145	25	4
53.60	0.09	97	12	4	282.49	0.26	95	24		480.43	0.29	98	24	
59.96	0.05	92	8		309.50	0.30	82	20		485.37	0.29	118	15	4
69.43	0.06	102	15		319.44	0.31	89	22		542.34	0.35	80	10	3
94.80	0.10	80	16		331.64	0.33	88	20		590.10	0.39	94	28	
107.57	0.12	82	8	3	335.14	0.34	91	16	4	612.71	0.42	93	20	
131.56	0.17	120	18	4	343.00	0.35	97	15	4					
157.78	0.22	75	16	3	346.50	0.36	86	18						

An advance in the analysis was made in a series of papers by Dyson alone,[2] and in collaboration with Mehta[2] where a new mathematically equivalent circular ensemble was introduced. For the relevant circular orthogonal ensemble (C.O.E.), the eigenvalues are treated as points on a unit circle, and the joint probability is proportional to the product of the chord lengths between all possible pairs of levels. They were able to show that a crystalline-like long-range order for the spacings is implied. In particular, their statistic Δ_3, which we denote simply Δ, is the mean square deviation between the "ladder function" $N(E)$ of (observed) levels vs E and a best-fit straight line:

$$\Delta \equiv \min_{A,B} \int_0^{\Delta E} (N - AE - B)^2 dE \,. \tag{4}$$

In the absence of long-range correlations, it is easy to show that Δ should increase linearly with the total number of levels n for $n \gg$ the spacing correlation length. On the basis of our own Monte Carlo calculations, we find

$$\langle\Delta\rangle \approx n/(55 - 210/n), \tag{5}$$

using 25 000 sets of 108 adjacent U.W. spacings and 15 000 sets each for various smaller numbers of adjacent U.W. spacings. The Δ distribution was quite widely spread out on either side of $\langle\Delta\rangle$. In contrast, Dyson and Mehta show[2] for their C.O.E. that

$$\langle\Delta\rangle = (1/\pi^2)(\ln n - 0.0687)\,, \tag{6a}$$

$$\mathrm{Var}\Delta = (0.11)^2\,. \tag{6b}$$

This remarkable formula implies that $n \sim 20\,000$ is needed before $\langle\Delta\rangle = 1.00$, showing the degree of long-range crystalline-like regularity predicted. The spread of Δ values for a U.W. distribution is such that there is more overlap with Eq. (6a) than is useful for a clean experimental rejection of the U.W. case for data agreeing with Eq. (6a), even for $n \sim 50$. It is useful also to consider the correlation coefficient for adjacent nearest-neighbor level spacings. We define

$$\rho(A,B) \equiv \frac{\langle (A - \langle A\rangle)(B - \langle B\rangle)\rangle}{[\langle (A - \langle A\rangle)^2\rangle \langle (B - \langle B\rangle)^2\rangle]^{1/2}}. \tag{7a}$$

TABLE XI. Predicted behavior of $\langle\Delta\rangle$ and $[\mathrm{Var}\,(\Delta)]^{1/2}$ as a function of the number of levels for Wigner's random matrix model and Dyson's circular ensemble. It is seen that for these tests the predictions of the two models are indistinguishable.

Monte Carlo random matrix calculations					Theoretical predictions of the circular ensemble	
No. of matrices diagonalized	Matrix dimension	Eigenvalues used	$\bar{\Delta}$	$[\mathrm{Var}\,(\Delta)]^{1/2}$	$\langle\Delta\rangle$	$[\mathrm{Var}\,(\Delta)]^{1/2}$
78	21	13	0.257 ± 0.011	0.098	0.253	0.11
78	31	23	0.324 ± 0.012	0.106	0.311	0.11
78	41	33	0.364 ± 0.014	0.124	0.347	0.11
78	50	42	0.372 ± 0.011	0.098	0.372	0.11
62	81	77	0.424 ± 0.012	0.094	0.433	0.11
900 [a]	120	109	0.470 ± 0.003	0.093	0.468	0.11

[a] Calculated using Dyson's Brownian-motion model.

For the orthogonal ensemble (O.E.) and large n, Mehta has shown that one expects to obtain a negative ρ for adjacent level spacings.

$$\rho(S_j, S_{j+1}) \approx -0.27 . \tag{7b}$$

We find that the sum of Δ and this quantity, abbreviated as $[\Delta + \rho]$, gives a considerably better separation of the predicted values for the U.W. and O.E. distributions than either Δ or ρ alone.

For the above comparison one needs to know not only the expected mean values for such parameters as Δ and ρ, but one must know the probability distributions for each n. Camarda[14] developed a computer program for generating and diagonalizing suitable $N \times N$ random Gaussian real square symmetric matrices, which would have eigenvalues obeying the Wishart distribution. This was carried out for 78 sets each for $N = 21$, 31, 41, 50, and 62 sets with $N = 81$. The eigenvalue distributions were found to be in satisfactory agreement with the Wigner semicircle law. A parameter transformation was made to unfold the semicircle form to constant density after two or more eigenvalues were omitted at each end to minimize end-effect errors. The resulting transformed eigenvalue distributions were then subjected to various statistical tests.

Values of $\langle \Delta \rangle$ and Var(Δ) were calculated and found, as expected, to agree with the DM result for the C.O.E., to within statistical uncertainties. We are not aware of any previous explicit demonstration of this equality using finite matrices.

Results for these random matrix calculations are given in Tables XI and XII. The calculations were performed using the IBM type 360-44 computer at Nevis, for which it is uneconomical to treat large numbers of matrices of larger dimensions. During discussions with Professor Dyson of our experimental results and the comparisons with the above theoretical analysis, he suggested that we try to make use of his Brownian-motion model[15] to simulate the behavior of larger random square matrices. One starts from Eqs. (17) and (18) of his paper[15] which can be written in the form

$$\langle \delta x_j \rangle = E(x_j)\delta t/f ,$$

$$\langle (\delta x_j)^2 \rangle = 2kT\delta t/f ,$$

where

$$E(x_j) = \frac{-x_j}{a^2} + \sum_i \frac{1}{x_j - x_{j-i}} ,$$

where i ranges from $-m$ to $+m$, excluding $i = 0$.

One selects an initial set of lattice points x_j, which can have an arbitrary distribution. In practice, it may be a lattice with constant unity spacings, or one using U.W. spacings. The procedure used to generate the new distribution is as follows:
(1) Set $kT = 1$ and mean point density = 1;
(2) divide the total number, $N + 4m$, of points into five adjacent groups containing m, m, N, m, and m adjacent points, where $m \approx N/2$. The outermost groups of m points are kept fixed, and the middle $m + N + m$ points are reevaluated from their initial values x_j^0 using

$$x_j^{n+1} = x_j^n + \sum \frac{\epsilon^2}{x_j^n - x_{j-i}^n} \pm 1.414\epsilon ,$$

where the sum over i is from $-m$ to $+m$ (excluding $i = 0$) and the sign ($\pm$) is chosen randomly. The convergence of the result is sensitive to the choice of the parameter ϵ, where $\epsilon^2 = \delta t/f$. Empirically, if $\epsilon \gtrsim 0.1$, the disturbance due to each iteration is too large to yield good results. If too small an ϵ is chosen, the convergence is too slow. In our successful procedure, after much experimentation with other choices, a value $\epsilon = 0.05$ was used. The iterations were performed with occasional tests using only the middle N points to calculate values of Δ_{DM} and of $\rho(S_j, S_{j+1})$. These values start far from their final values and "walk" towards their equilibrium values with a superimposed "jitter." The idea is to continue the iteration until, except for the jitter, equilibrium seems to have been

TABLE XII. Tabulated below are the average values of $\rho(S_i, S_{i+1})$ calculated using the average sample spacing $\bar{S}$ and the true average spacing $\langle S \rangle$. The difference between the values of $\langle \rho(S_i, S_{i+1}) \rangle$ obtained using $\bar{S}$ and $\langle S \rangle$ (for the same number of levels) is much less than the difference $1/n$ found in the uncorrelated case.

No. of matrices diagonalized	Matrix dimension	Eigenvalues used	$\langle \rho(S_i, S_{i+1}) \rangle_{\bar{S}}$	$\langle \rho(S_i, S_{i+1}) \rangle_{\langle S \rangle}$
78	21	15	-0.250 ± 0.026	-0.236 ± 0.026
78	31	25	-0.241 ± 0.021	-0.233 ± 0.021
78	41	35	-0.269 ± 0.018	-0.266 ± 0.018
78	50	44	-0.274 ± 0.016	-0.272 ± 0.016
62	81	77	-0.256 ± 0.012	-0.256 ± 0.012
900 [a]	120	109	-0.277 ± 0.003	-0.276 ± 0.003

[a] Calculated using Dyson's Brownian-motion model.

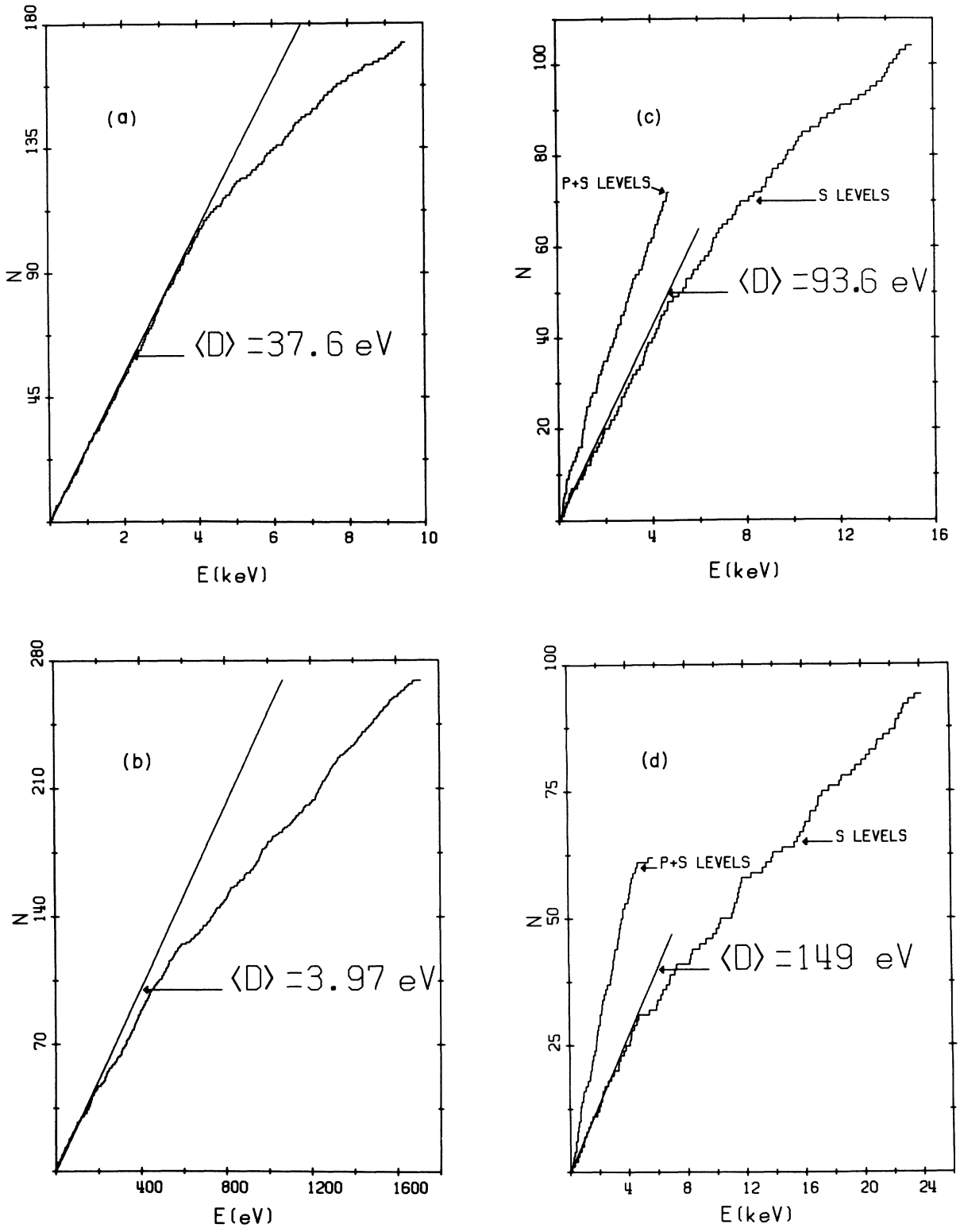

FIG. 4. Plots, N vs E, of number of observed levels vs energy for (a) Er^{166}, (b) Er^{167}, (c) Er^{168}, (d) Er^{170}. The values of $\langle D \rangle$ shown in plots represent the slopes of visually fitted straight lines. The optimum evaluation of $\langle D \rangle$ values for various erbium isotopes is discussed in text.

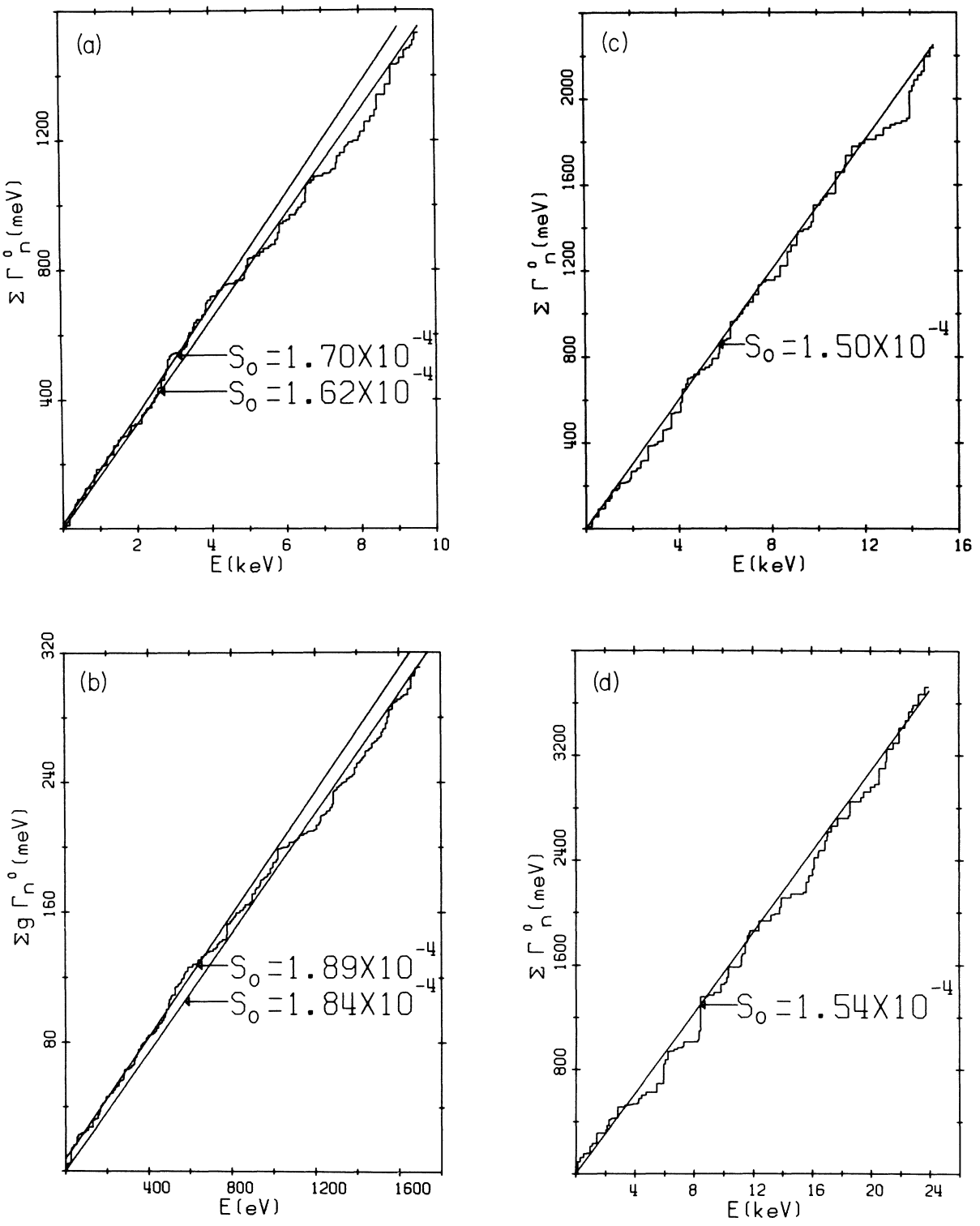

FIG. 5. Plots of $\sum \Gamma_n^0$ (or $g\Gamma_n^0$) vs energy for (a) Er^{166}, (b) Er^{167}, (c) Er^{168}, and (d) Er^{170}. The slopes give the s-wave strength functions.

reached. This required ~1500 iterations. The central N points were then listed as a first set of results. Subsequently, sets of ~25 iterations were performed using $\epsilon = 0.025$, to minimize jitter contribution to Δ, until a suitably large number of output sets of N points were obtained. Each set is *not* independent of the one before (using 25 iterations, $\epsilon = 0.025$). However, the large number of sets covers the range of variation adequately, and it is easy to generate large numbers of sets once the first has been obtained.

Special procedures are required in the above iteration in two special cases as follows: When two points are so close together that $1/(x_j - x_{j\pm1})$ is too large, the maximum change $|x_j^{n+1} - x_j^n|$ is limited to some maximum value which we chose to be 0.15. The second crisis comes when the motion of one point is through another point. In this case, we simply relabeled the points to maintain a monotonic ordering.

The detailed evolution of these procedures began with suggestions by Professor Dyson, with modifications introduced by Dr. H. Camarda in the process of trying to achieve successful results. The results were equivalent to diagonalizing 900 sets of $N = 120$ matrices. The results are included at the bottom of Tables XI and XII. In addition, these calculations yielded a result for the nearest-neighbor level spacing distribution of sufficient statistical accuracy that it was in agreement with Gaudin's[12] more exact evaluation, which is slightly different from the Wigner distribution, Eq. (1).

In addition to the statistical tests for level spacing distributions discussed in this paper, there is a different statistical test developed by Rosenzweig and Monahan.[16] This test also shows good behavior for Er^{166}. We have communicated the erbium and some other results to Rosenzweig and Monahan so they could present their analysis and interpretation in an accompanying article.[17] We also omit here, for presentation in an accompanying article,[6] the results of additional analysis suggested by Professor Dyson.

VII. DISCUSSION OF RESULTS – COMPARISON WITH THEORIES

The results for N vs E, the cumulative level count vs energy over the ranges of Tables II to VII, are shown in Figs. 4(a)–4(d). For Er^{166}, it is seen that the cumulative number of levels is almost perfectly linear to 4200 eV, followed by an abrupt curving away to a lower slope. In our subsequent analysis for statistical fits, we use either the first 4200-eV region, or the first 3-keV region, as discussed below. Figure 4(b) shows that Er^{167} has a much higher level density, as is expected for an odd-A nucleus. The original slope for the first 120 eV is followed by a gradually decreasing slope, though there seems to be a grouping into three regions of roughly constant slope for 0–120, 120–600, and 600–1700 eV. The break

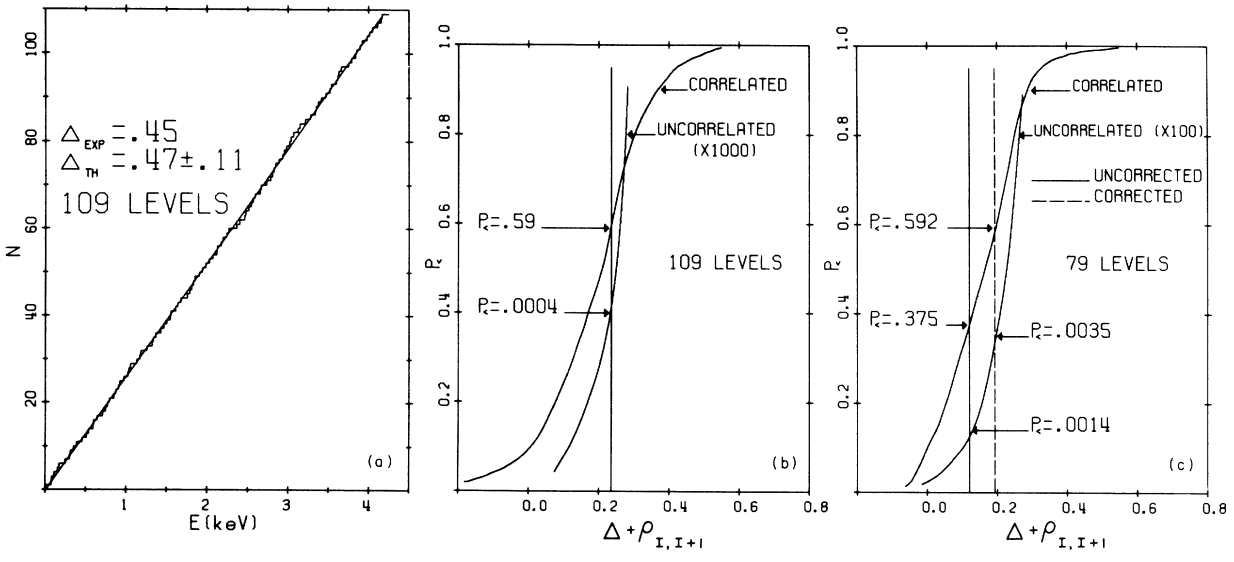

FIG. 6. (a) Best straight-line fit to N vs E for all 109 observed resonances in Er^{166} to 4200 eV. This gives $\Delta = 0.455$ for Dyson's parameter. (b) A plot of the probability of obtaining $\leq$ the indicated value of $\Delta + \rho(S_j, S_{j+1})$ for a set of 108 adjacent spacings, for uncorrelated Wigner adjacent spacings, and when correlations are included according to O. E. theory. The experimental result for Er^{166} is indicated. (c) Same as Fig. 6(b) for the 78 (or 79) adjacent spacings of Er^{166} to 3 keV. The experimental values are obtained as discussed in the text.

TABLE XIII. Summary of the results for statistical test on the spacings. Level choices A and C for Er^{168} and Er^{170} are as in Tables IV–VII. Choice B treats the 3751.6 Er^{168} level as p. Choices D, E, and F for Er^{170} treat the 598.2-eV level as p, the 975.0-eV level as p, and *both* as p, respectively.

Isotope	Level choice	E_{max} (keV)	n	Δ_{D-M}	Δ_{exp}	$\rho(S_j, S_{j+1})$	$(\Delta+\rho)$	$P_<$(O.E.)	$P_<$(U.W.)
166	all	4.2	109	0.468	0.455	-0.220	0.235	0.590	0.0004
166	all	3	79	0.436	0.373	-0.253	0.120	0.375	0.0014
166	Mod.	3	80	0.437	0.400	-0.207	0.193	0.592	0.0035
168	A	4.7	50	0.389	0.287	-0.295	-0.008	0.180	0.0035
168	B	4.7	49	0.387	0.302	-0.275	+0.027	0.200	0.006
170	C	4.8	31	0.341	0.359	-0.093	0.266	0.780	0.230
170	D	4.8	30	0.338	0.322	-0.035	0.287	0.810	0.252
170	E	4.8	30	0.338	0.269	-0.129	0.140	0.575	0.122
170	F	4.8	29	0.334	0.325	-0.062	0.263	0.780	0.227

at 600 eV is probably due to its being the upper energy for which self-indication analysis was used for Er^{167}. The Er^{168} data plot in Fig. 4(c) shows all observed levels to 4700 eV. Although we have no experimental signature to distinguish weak levels as s or p, a Bayes-theorem analysis, described below, gave a separation of resonances most apt to be p levels. Figure 4(c) also shows the level count to 15 keV for the remaining "s levels." The 4700-eV limit is where the analysis of the self-indication data was stopped. For Er^{170}, Fig. 4(d), a similar procedure has been used, i.e., all levels are shown to 4800 eV and those *not* deleted as "probable p levels" to 24 keV. The self-indication analysis was stopped at 4800 eV.

Figures 5(a)–5(d) show the corresponding plots of $\sum\Gamma_n^0$, or $\sum g\Gamma_n^0$ for the evaluation of the S_0 values. In these plots, it is not important if weak levels are missed. The straight lines represent average slopes, except where separate slopes are

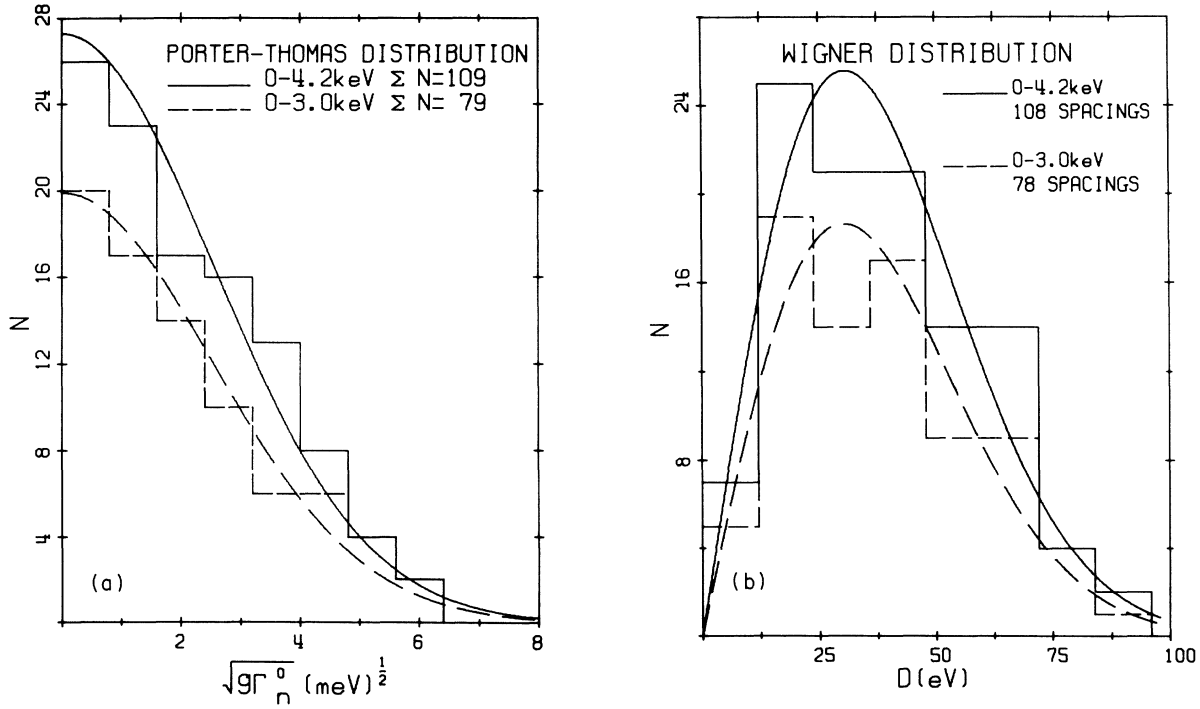

FIG. 7. (a) Plot of the distribution of $(\Gamma_n^0)^{1/2}$ values for Er^{166} to 4.2 and to 3 keV. The Porter-Thomas curves are shown for comparison. (b) Plot of the adjacent spacing distribution for Er^{166} to 4.2 and to 3 keV and the comparison Wigner distribution curves. All experimental levels are included.

also shown for the lower-energy parts of the range, which are believed to be of somewhat greater experimental reliability. The values of S_0 obtained are listed below with fractional-uncertainty values of $(2/n)^{1/2}$:

Er^{166}: $10^4 S_0 = \begin{cases} 1.62 \pm 0.17 & \text{full range,} \\ 1.70 \pm 0.23 & \text{selected range;} \end{cases}$

Er^{167}: $10^4 S_0 = \begin{cases} 1.84 \pm 0.16 & \text{full range,} \\ 1.89 \pm 0.20 & \text{selected range;} \end{cases}$

Er^{168}: $10^4 S_0 = 1.50 \pm 0.21$ full range, *and* favored value;

Er^{170}: $10^4 S_0 = 1.54 \pm 0.22$ full range, *and* favored value.

For the 109 levels to 4200 eV for Er^{166}, the DM best-fit straight line to $N(E)$ is shown in Fig. 6(a). It gives $\Delta_{\mathrm{exp}} = 0.455$ vs $\Delta_{\mathrm{DM}} = 0.468 \pm 0.11$, $\langle D \rangle = 38.3$ eV. The fractional uncertainty in $\langle D \rangle$ is expected to be $\sim 1/n$ for O.E. theory. For the same region, we obtain $\rho(S_j, S_{j+1}) = -0.22$, which is also in good agreement with the O.E. predicted value of $\sim -0.27 \pm 0.09$ for this sample size. The standard deviation for $\rho(S_j, S_{j+1})$ for the O.E. theory is $\approx 0.92/(n-1)^{1/2}$. We list the observed $\rho(S_j, S_{j+1})$ values *without* uncertainties, comparing with the predicted values with n-dependent uncertainties.

While the above experimental values are in excellent agreement with O.E. predictions, it is important to see if they also agree or disagree with otherwise "reasonable" alternate theories which do not contain correlation effects. It is *not* reasonable to compare with a theory of randomly spaced levels which predicts very large Δ values, since the Wigner distribution is known to give a good description for the nearest-neighbor spacings. We thus compare with a U.W. distribution and use as our test the probability of achieving less than or equal to the observed values. Since a more sensitive test is obtained using $\Delta + \rho(S_j, S_{j+1}) \equiv [\Delta + \rho]$ than Δ or ρ alone, this comparison has been made using the Monte Carlo calculation results described in the preceding section. The results are shown in Table XIII and in Fig. 6(b). The corresponding results for all of the 79 levels of Er^{166} to 3 keV are also shown in the table, and in Fig. 6(c). The observed values of Δ, ρ, and $[\Delta + \rho]$ are in good agreement with O.E. predictions, but the probability for $\leq$ the observed value is only 0.0004 to 4.2 and 0.0014 to 3 keV for the U.W. case.

It should be noted that the mean of $\rho(S_j, S_{j+1})$ is not zero for a finite sample when there are no *a priori* correlations. This occurs, since one uses the sample mean rather than the true mean, and this bias leads to $\rho \approx -1/n \pm (1/n)^{1/2}$ for n spacings, for n not too small. This effect is most easily seen in the simple case of $n = 2$ where one always obtains $\rho(S_j, S_{j+1}) \equiv -1$.

While these results are in excellent agreement with O.E. theory, a single s-level population should also show agreement with the Wigner formula for the nearest-neighbor spacing distribution and with the PT single-channel theory for the distribution of Γ_n^0 values [or $(\Gamma_n^0)^{1/2}$]. The comparisons, shown in Figs. 7(a) and 7(b), yield excellent fits to the theoretical curves both to 4.2 and to 3 keV.

The measurements for Er^{168} and Er^{170} contain a large excess of weak levels relative to the PT theory. This is shown in Figs. 8(a) and 9(a) which imply ~22 extra weak levels for Er^{168} and 30 for Er^{170} to 4.7 and 4.8 keV, respectively. A very few of these most marginal levels may be spurious "noise" fluctuations, but most are probably due to the inclusion of a partial p-level population. There is also the problem that a few very weak s levels may have been missed. The situation has been examined quantitatively by considering the threshold sensitivity for "observing" resonances (over background noise fluctuations) as a function of energy for the various measurement conditions. Since S_0 and $\langle D \rangle$ are relatively well established from the main groups of nonweak s levels, we can calculate *how many* s levels in each energy interval are expected to be weaker than threshold, and thus obtain estimated mean values for missed s levels. The predicted number of p levels which would be observed depends on the assumed p strength function S_1, and the true p-level density, which we take to be 3 times that for s levels. Since the expected number of observed p levels is a rapidly increasing function of assumed S_1, a comparison with the observed excess of weak levels plus the calculated mean for missed weak s levels gives an evaluation of S_1 and an estimate of its uncertainty in each case. For Er^{168} and Er^{170}, the following analyses give definite indications as to which are most apt to be p levels. The separations into s and p levels in Tables IV–VII were made this way. (A *few* of these assignments may be incorrect.) The number of levels subtracted as "p levels" was *chosen* to give a good fit to the PT theory for the $(\Gamma_n^0)^{1/2}$ values as shown in Figs. 8(a) and 9(a). The nearest-neighbor level spacing distributions before and after the "corrections" are shown in Figs. 8(b) and 9(b). It is seen that the fits to the theoretical curves are good in each case for the "corrected s-level sets."

The corresponding DM straight-line fit to the selected s-level populations, with the indicated

comparisons of chosen s population and O.E. predicted Δ values are shown in Figs. 8(c) and 9(c). Figures 8(d) and 9(d) show the probabilities of obtaining $\leq$ the observed $[\Delta+\rho]$ values for the O.E. theory and for a U.W. spacing set having the observed numbers of spacings. The agreement is, in both cases satisfactory for the O.E. comparison. For Er^{168}, there is a very small probability of achieving the chosen s-population $[\Delta+\rho]$ value for a U.W. set. Before making more detailed comments on these "selected s-population" results, we present the details of the selection procedure below.

A careful study of the data analysis gives the

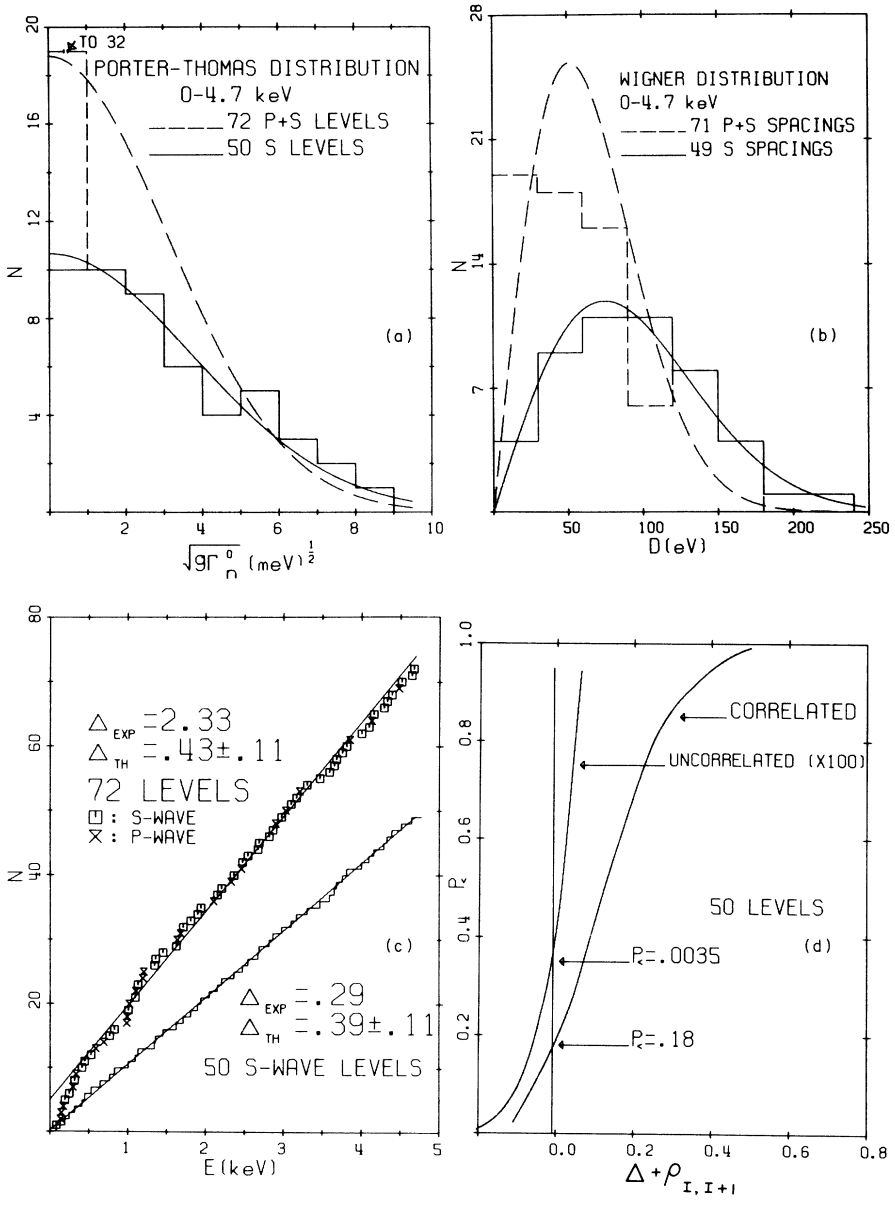

FIG. 8. (a) Distribution of $(\Gamma_n^0)^{1/2}$ values for Er^{168} to 4.7 keV, using all of the levels, and excluding 22 weak levels (p wave). (b) Nearest-neighbor level spacing distribution for Er^{168} to 4.7 keV compared with the Wigner distribution. The dashed lines correspond to all levels, while the solid lines are for our selected s levels (choice A of Table XIII). (c) Comparisons of N vs E with the best fitting straight lines for Dyson's Δ test. Er^{168} to 4.7 keV as in (b). (d) Same as Fig. 6(b) for the 49 Er^{168} spacings of choice A of Table XIII to 4.7 keV, for s levels only as discussed in the text.

following threshold sensitivities for level "detection":

For Er^{166}:

Flat detector $(\Gamma_n)_{min} \approx 16\times10^{-5}\ [E/(1\text{ eV})]^{1.5}$ meV,

Self-indication $(\Gamma_n)_{min} \approx 3.7\times10^{-5}\ [E/(1\text{ eV})]^{1.5}$ meV.

For Er^{168}:

Flat detector $(\Gamma_n)_{min} \approx 28\times10^{-5}\ [E/(1\text{ eV})]^{1.5}$ meV,

Self-indication $(\Gamma_n)_{min} \approx 3.4\times10^{-5}\ [E/(1\text{ eV})]^{1.5}$ meV.

For Er^{170}:

Flat detector $(\Gamma_n)_{min} \approx 16\times10^{-5}\ [E/(1\text{ eV})]^{1.5}$ meV,

Self-indication $(\Gamma_n)_{min} \approx 3.1\times10^{-5}\ [E/(1\text{ eV})]^{1.5}$ meV.

The $E^{1.5}$ power law is the same as the p-level energy dependence for Γ_n, so except for resolution difficulties at higher energies, the probable density of p levels *seen* should be energy-independent, while the probability of missed weak s levels increases with the following estimate:

	0–1000 eV	1000–2000 eV	2–3 keV	3–4 keV	4–4.7, 4.8 keV
Er^{166}	1.05	1.91	2.47	6.	...
Er^{168}	0.27	0.50	0.65	0.77	0.60
Er^{170}	0.13	0.24	0.31	0.36	0.32

It is seen that a nontrivial number of s levels are probably missed for Er^{166}, but only ~2 for Er^{168} and 1 for Er^{170}.

For Er^{168} and Er^{170}, a comparison of expected number (mathematical expectation) of observed p-wave levels, vs *assumed* p-wave strength function S_1 with the actual observed excess of weak levels (24 for 168) and (30 for 170), establishes the "best" values for S_1, as well as uncertainty limits (using $R = 7.72\times10^{-13}$ cm for the nuclear radius):

Er^{168}: $10^4 S_1 = 0.70 \pm 0.20$,

Er^{170}: $10^4 S_1 = 0.80 \pm 0.25$.

To obtain a proper fit of the observed $(\Gamma_n^0)^{1/2}$ distribution to the PT function for Er^{166}, approximately the same number of p levels should have been included as weak s levels missed. This gives a best S_1. An upper limit for S_1 can also be obtained as one giving *distinctly too many weak* levels:

Er^{166}: $10^4 S_1 \lesssim 0.75$,

with 0.60 as the "best estimate" value.

We have followed the method of the Argonne group in their U^{238} analysis.[18] Assuming an *a priori* level density proportional to $2J+1$, there should be 3 times as many p levels as s levels. Using all but the low end of the $(\Gamma_n^0)^{1/2}$ distribution, a best fit of the experimental histogram can be made. This yields a $\langle D\rangle$ for s levels, and thus $\frac{1}{3}$ this value for p levels. Then for any assumed S_1 and the observed S_0, one can use a Bayes-theorem calculation of *a posteriori* probability that each observed weak level is s or p wave (using *a priori* values of $\frac{1}{4}$ and $\frac{3}{4}$), in addition to the expectation for missed s and observed p levels. Table XIV shows the results of this calculation using $S_1 = 0.6\times10^{-4}$ for the first 3 keV for Er^{166}. Since the absence of self-indication data above 3 keV increases the expectation for missed s levels in the 3-to-4.2-keV region, the data to 3 keV, in principle, provides a "cleaner" test set.

A. Er^{166} (0–3 keV)

There were four levels having $p \geq 0.58$ *a posteriori* probability from the Bayes-theorem analysis as being p wave (using $S_1 = 0.6\times10^{-4}$). These were considered to be p levels. The remaining weak levels had $p \leq 0.13$ for being p and these were treated as being s. Five "missed" s levels were added using two guides: (a) the number per keV suggested by the previously mentioned expectation for the number of missed s levels/keV; (b) where removing "p levels" gave an unlikely large nearest-neighbor spacing, when compared with the Wigner distribution, a "missed s level" was inserted at the *center* of the interval to not bias the $\rho(S_j, S_{j+1})$ value. This only happened once for a 117.3-eV interval centered at 1699 eV. The other four were placed where spacings of 65.5, 72.4, 79.6, and 95.0 eV occurred, two where "p levels" had been removed. The other two were arbitrarily at the two largest remaining spacings. The "inserted" "missed" weak s levels were placed at 118.0, 1292, 1699, 2317, and 2696 eV. While there is some arbitrariness, the criterion was not chosen to minimize Δ or $\rho(S_j, S_{j+1})$.

The results for the 0–3-keV region after doing this are given in Table XIII. It is seen that Δ is slightly increased and $\rho(S_j, S_{j+1})$ is made a little less negative. The fit of the nearest-neighbor

spacing distribution to the Wigner shape is not significantly changed. The opposite sign of the changes after "corrections" shows that the changes were not "fudged" to yield better fits. In the absence of a more reliable specific test for s vs p character for these very weak levels, it is probably better to emphasize the use of the "uncorrected" level population for Er^{166}, noting that *a priori*, one expects to obtain higher Δ values and less negative $\rho(S_j, S_{j+1})$ when the population is incomplete and/or contaminated.

B. Er^{168} (0-4.7 keV)

The 32 weakest levels of Er^{168} were similarly analyzed using Bayes's theorem with $10^4 S_0 = 1.5$ and $10^4 S_1 = 0.7$. Then *a posteriori* probabilities were obtained for the probability of each level

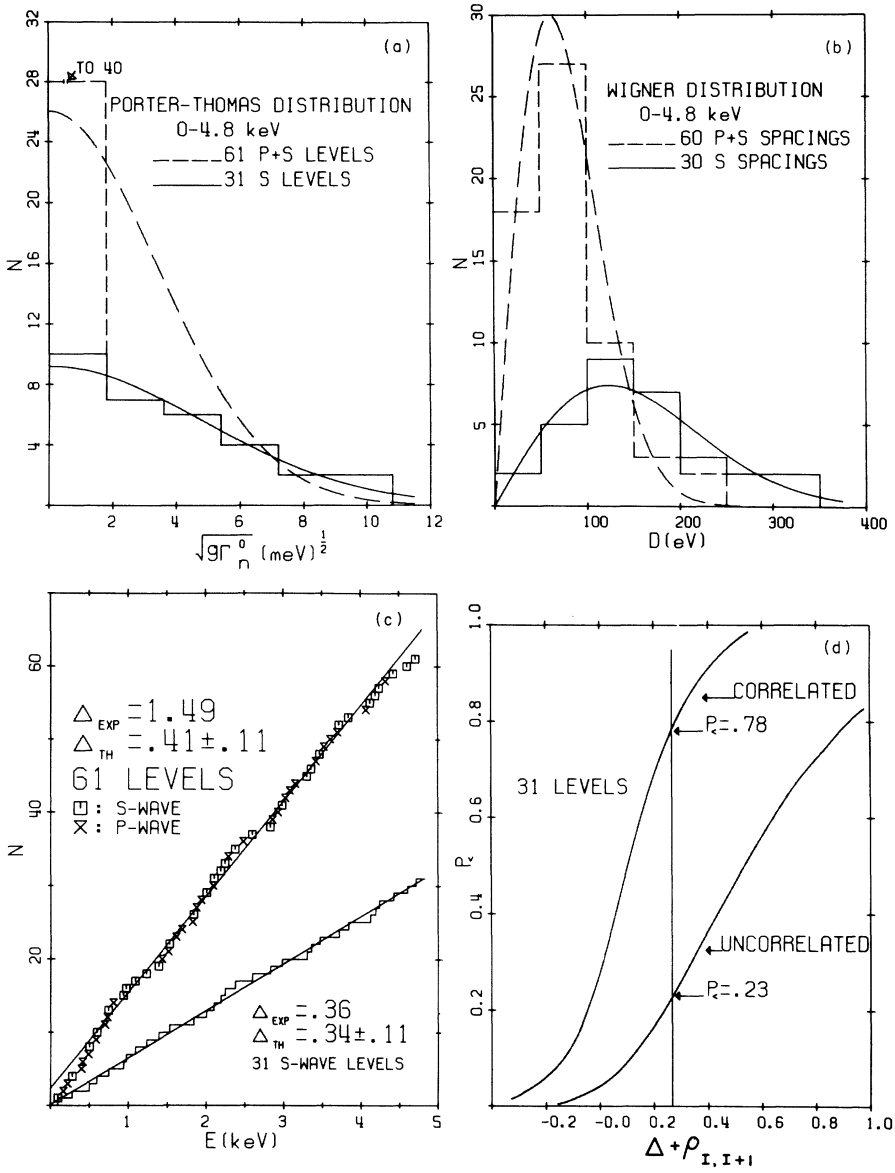

FIG. 9. (a) Distribution of $(\Gamma_n^0)^{1/2}$ values for Er^{170} to 4.8 keV and comparison with the Porter-Thomas distribution. The dashed curves include all resonances while the solid ones are for those chosen as s levels. (b) Nearest-neighbor level spacing distribution for Er^{170} to 4.8 keV compared with the Wigner distribution using all levels and using our s-level selection (choice C of Table XIII). (c) Comparisons of N vs E with the best fitting straight lines for Dyson's Δ test. Er^{170} to 4.8 keV as in Figs. 9(a) and 9(b). (d) Same as Fig. 6(b) for the 30 Er^{170} spacings (choice C of Table XIII) to 4.8 keV, for the selected s levels only.

being p. The results are shown in Table XV. The 24 levels denoted by superscript a were considered to be p levels. They mainly had p probabilities ≥ 0.9 (19 levels), with the remaining five having probabilities 0.859, 0.839, 0.830, 0.792, and 0.587. The eight levels chosen as s had p probabilities <0.20 for five and 0.385, 0.395, and 0.607 for the other three. The separation is very great for all but the "p level" with 0.587 probability and the "s level" with 0.607 probability. This last p-level choice was to avoid a concentration of three of the eight s choices in the 2500-to-3000-eV region. The "s level" at 3751.6 eV (0.607 p probability) was included to give 10 levels in the weakest $(\Gamma_n^0)^{1/2}$ box of Fig. 8(a) after two more "missed" s levels are added as suggested by the preceding analysis for the expected number of missed s levels. These "missed s levels" were added at 646 and at 2045 eV to split the two largest spacings and were retained for all "s population" selections for Er^{168}.

Inclusion of the level at 3751.6 eV as an "s level" is somewhat arbitrary, since the Bayes analysis is "cleaner" if it is also taken as a p level, so all levels chosen as p levels have p probabilities ≥ 0.587, and all levels in Table XV considered to be s have ≤ 0.395 p probability.

Table XIII shows the various results and comparison with theory for the two ways of choosing: A, treating the 3751.6-eV level as s; B, treating the level as p. While Figs. 8(a) and 8(b) are for choice A, the fits are essentially equally good for choice B. Similarly, the fits of Δ, $\rho(S_j, S_{j+1})$, and $[\Delta + \rho]$ to the O.E. case is essentially as before, with a slightly weaker rejection of the U.W. case. The $(g\Gamma_n^1)^{1/2}$ distribution for choice A is shown in Fig. 10. It gives a good fit to the high end of the expected PT distribution for $10^4 S_1 = 0.70$.

TABLE XIV. Bayes-theorem results for the weak levels of Er^{166} to 3 keV; $S_0 = 1.7 \times 10^{-4}$, $S_1 = 0.6 \times 10^{-4}$.

E_0 (eV)	Γ_n^0 (meV)	$g\Gamma_n^1$ (meV)	Prob. (p)
15.56	0.55	12 200	0.000
110.63 [a]	0.006	18.8	0.826
154.15	0.56	1270	0.000
457.88	0.07	53	0.001
601.01	0.17	99	0.000
708.29	0.105	52	0.001
873.07	0.22	89	0.000
923.90	0.08	30	0.132
973.94	0.08	30	0.129
1036.9	0.25	82	0.000
1325.0	0.13	34	0.049
1431.3	0.2	49	0.002
1545.6 [a]	0.07	16.6	0.671
1618.1	0.17	36	0.030
1678.9 [a]	0.09	18.3	0.580
1906.5	0.23	42	0.008
2069.0	0.18	30	0.088
2548.5	0.24	33	0.047
2669.6 [a]	0.10	12.7	0.787
2850.2	0.56	69	0.000

[a] Levels considered to be $l = 1$.

C. Er^{170} (0–4.8 keV)

The 40 weakest Er^{170} levels were similarly analyzed by a Bayes-theorem method using $10^4 S_0 = 1.54$ and $10^4 S_1 = 0.8$. The results are shown in Table XVI. The 30 levels subtracted as "p levels" had ≥ 0.785 probability of being p, with all but two ≥ 0.85 probability. The remaining 10 levels considered to be "s levels" had <0.45 probability of being p except for two having 0.63 probability.

TABLE XV. Bayes-theorem results for the weak levels of Er^{168} to 4.7 keV; $S_0 = 1.5 \times 10^{-4}$, $S_1 = 0.7 \times 10^{-4}$.

E_0 (eV)	Γ_n^0 (meV)	$g\Gamma_n^1$ (meV)	Prob. (p)
139.58 [a]	0.0093	23	0.975
145.71 [a]	0.0051	12	0.989
174.29 [a]	0.0114	23	0.973
296.67 [a]	0.0168	20	0.972
335.47 [a]	0.046	48	0.792
410.82	0.099	83	0.194
445.96	0.109	85	0.172
587.34 [a]	0.020	12	0.978
691.46 [a]	0.038	19	0.959
985.73 [a]	0.064	23	0.938
990.61 [a]	0.079	28	0.910
1022.4 [a]	0.054	18	0.954
1106.1 [a]	0.117	37	0.830
1193.2 [a]	0.064	19	0.949
1207.7 [a]	0.075	22	0.937
1342.8	0.24	63	0.384
1636.4 [a]	0.109	23	0.918
1681.3 [a]	0.073	15	0.953
2100.6 [a]	0.179	30	0.859
2325.9 [a]	0.089	13	0.952
2456.6 [a]	0.107	15	0.944
2544.0	0.58	79	0.121
2862.6	0.60	73	0.169
2900.5 [a]	0.39	47	0.587
3027.4 [a]	0.25	29	0.839
3202.8 [a]	0.15	16	0.931
3751.6	0.47	44	0.607
3849.9 [a]	0.23	21	0.900
4127.0 [a]	0.20	17	0.918
4284.3	0.93	76	0.116
4476.8 [a]	0.21	16	0.919
4643.6	0.72	54	0.395

[a] Considered to be $l = 1$.

This selection, denoted choice C in Table XIII, gives a "clean" separation and gives about the proper number of levels in the lowest $(\Gamma_n^0)^{1/2}$ box of Fig. 9(a) to give an over-all good fit to the PT single-channel curve. The $N(E)$ vs E before and after this p-level subtraction are shown in Fig. 9(c). If the levels at 598.2 and/or 975.0 eV are also treated as being p levels, choices D, E, and F, defined below, give results which are also presented in Table XIII:

Choice D: level at 598.2 eV considered p,
Choice E: level at 975.0 considered p,
Choice F: both levels considered p.
Choice F also gives a "clean" division of p probability for levels chosen as s or p.

It is seen that $\Delta_{\exp}$ and Δ_{DM} agree well for all choices, and $\rho(S_j, S_{j+1})$ is a little more consistent with zero than with −0.27 for all choices above. The $[\Delta+\rho]$ test shown in Fig. 9(d) is for choice C of Table XIII, and is not greatly changed for the alternate choices above. The Γ_n^0 distribution, Fig. 9(a), would give a good fit in all cases, as would the spacing distribution fit in Fig. 9(b). Mainly, one concludes that the Δ values for Er^{170} give a good fit to the O.E. value, but N is too small to exclude strongly the U.W. case. The Er^{166} and Er^{168} cases provide very much better tests of O.E. vs U.W. theory.

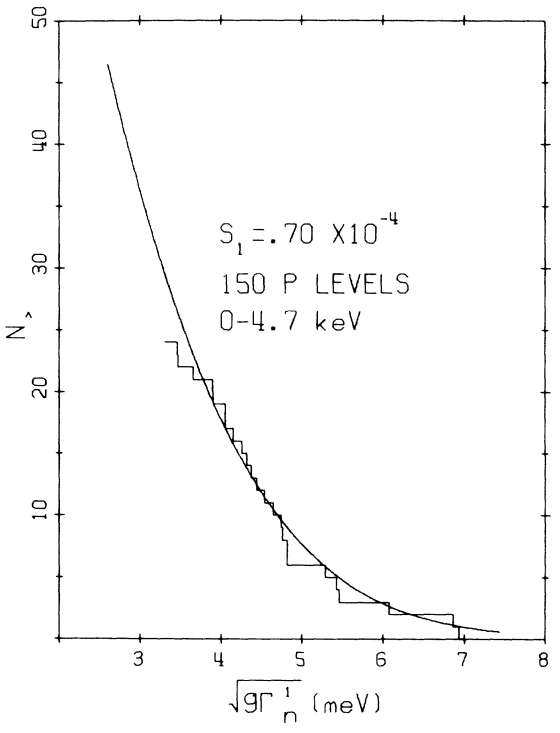

FIG. 10. Distribution of $(g\Gamma_n^1)^{1/2}$ values for those Er^{168} levels chosen as p levels for choice A of Table XIII. The best fit Porter-Thomas integral curve (from Bayes-theorem analysis) is shown.

D. Er^{167} Analysis

An examination of Fig. 4(b) of N vs E for Er^{167} shows an initial slope corresponding to $\langle D\rangle \approx 4.0$ eV. Since $I = \frac{7}{2}$ for the target nucleus, the s levels having $J = 3$ and $J = 4$ should have nearly equal abundances. This largely removes the Wigner repulsion effect against small nearest-neighbor level

TABLE XVI. Bayes-theorem results for the weak levels of Er^{170} to 4.8 keV; $S_0 = 1.54 \times 10^{-4}$, $S_1 = 0.8 \times 10^{-4}$.

E_0 (eV)	Γ_n^0 (meV)	$g\Gamma_n^1$ (meV)	Prob. (p)
164.59 [a]	0.0051	11	0.992
221.91 [a]	0.048	75	0.885
394.31 [a]	0.027	24	0.978
408.93 [a]	0.064	55	0.928
483.76 [a]	0.043	31	0.968
584.12 [a]	0.095	57	0.908
598.18	0.172	100	0.629
698.18 [a]	0.068	34	0.958
729.50 [a]	0.082	39	0.948
809.18 [a]	0.034	14.7	0.979
975.00	0.26	94	0.630
1230.7	1.08	307	0.000
1433.2 [a]	0.077	19	0.967
1512.1 [a]	0.22	50	0.888
1524.0	1.82	416	0.000
1618.1 [a]	0.085	18	0.966
1693.4 [a]	0.141	29	0.947
1827.6 [a]	0.28	54	0.864
1844.1	0.58	110	0.391
1874.9 [a]	0.28	52	0.872
1938.9 [a]	0.15	27	0.949
2087.2 [a]	0.081	14	0.968
2190.9	1.13	181	0.033
2291.0 [a]	0.33	51	0.863
2482.3 [a]	0.28	40	0.906
2594.0	0.75	101	0.445
2857.3 [a]	0.51	62	0.785
2928.0 [a]	0.176	21	0.950
3018.6 [a]	0.38	44	0.879
3083.4 [a]	0.36	41	0.892
3150.3 [a]	0.27	30	0.927
3352.8	0.95	99	0.428
3414.7 [a]	0.58	60	0.785
3518.1 [a]	0.123	12.3	0.961
3599.7 [a]	0.47	46	0.864
3698.0 [a]	0.153	14.5	0.956
3715.9	1.92	181	0.025
4067.4 [a]	0.14	12.2	0.958
4318.8 [a]	0.55	45	0.858
4599.6	1.59	122	0.207

[a] Considered to be $l = 1$.

spacings. Combined with the much smaller net $\langle D \rangle$ than for the even-A nuclei, the upper energy for which most resonances are resolved is greatly reduced. Also, if a $J=3$ and $J=4$ level are nearly coincident, they will be treated as a single level even where the instrumental resolution is quite good. Er^{167} does not provide a strong test of statistical theories where one must not miss s levels, or include p levels. When compared with the recent lower-resolution results of Mughabghab, Chrien, and Bhat,[9] we note that they resolved all but the 62.07-eV level to ~95 eV, after which they miss a large fraction of the levels which we observed. Their $g\Gamma_n^0$ values are in fair agreement for resonances which do not prove to be multiple.

Figure 5(b) shows that $\sum g\Gamma_n^0$ vs E is less influenced by missing levels, with a decreased slope being obvious mainly above 1 keV. The evaluation of S_0 mainly uses results to 1 keV for $S_0 = 1.89 \times 10^{-4}$. The comparison of the results to 118 eV (including the two levels below 1 eV) with the Wigner and PT functions are shown in Figs. 11(a) and 11(b). It is seen that we have about the correct number of weak levels. The highest histogram box in Fig. 11(b) is due to the resonance at 26.24 eV which has $(g\Gamma_n^0)^{1/2} = 2.794$, which is at the upper end of the last histogram box. For the first 118 eV, using the best fit PT curve, we expect only 0.04 levels having $\geq$ this $g\Gamma_n^0$ value. An obvious consideration is to investigate the possibility of an overlap of two relatively strong resonances of different J at this energy. Since the experimental resolution is very good at this energy, the separation of the E_0 values could be no greater than ~0.2 eV. The $g\Gamma_n^0$, Γ analysis for this level, similar to those of Fig. 3(a)–3(d), gives an excellent intersection of many different thick, thin, etc., flat detector and self-indication curves having a very wide range of slopes at the point of intersection. This is quite incompatible with a significant change in $\sum g\Gamma_n^0$ even for two coincident strong levels. The spacing distribution agrees reasonably well with that expected for two merged populations, each obeying the Wigner single-population nearest-neighbor spacing distribution, having level densities in the ratio 9 to 7.

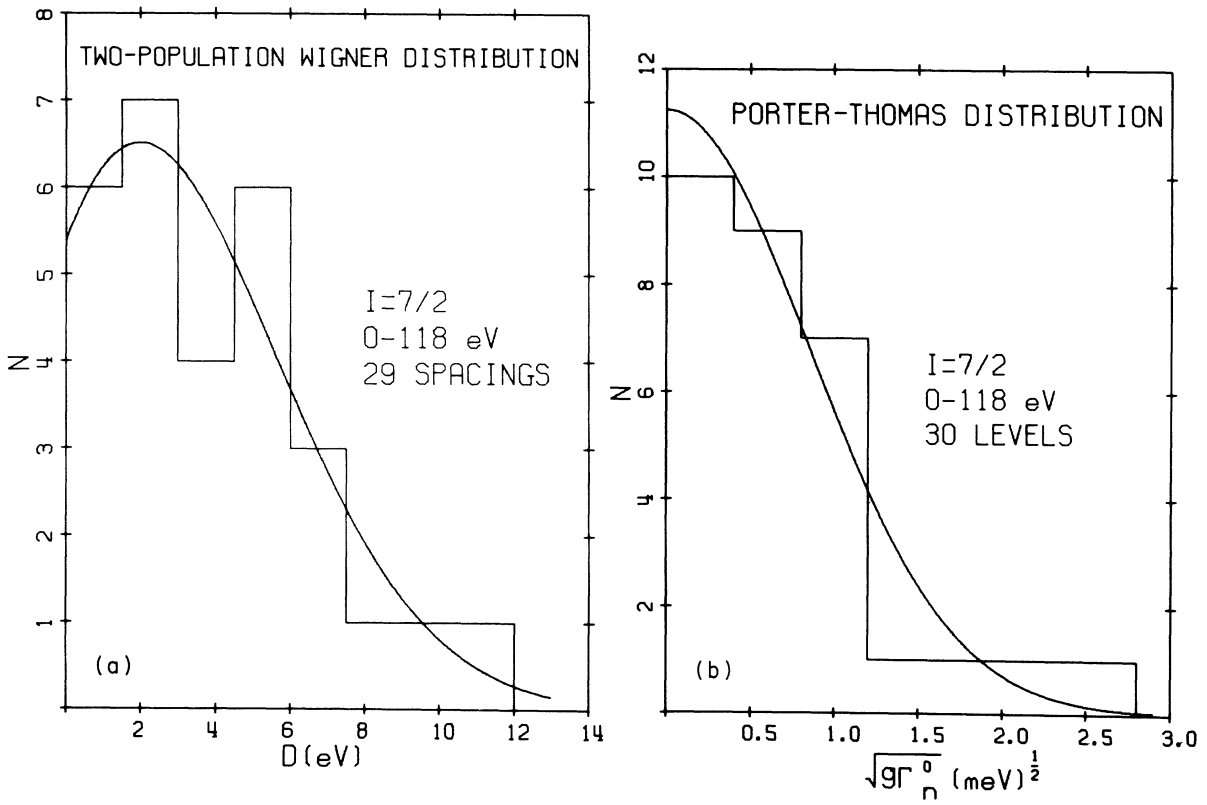

FIG. 11. (a) Adjacent level spacing distribution for the 29 spacings of Er^{167} below 118 eV. The curve is the expected resulting distribution expected if the $J=3$ and 4 compound states each separately follow the Wigner distribution, and the two populations are randomly mixed, with relative separate $\langle D \rangle$ values inversely as $(2J+1)$. (b) The observed distribution of $(g\Gamma_n^0)^{1/2}$ values for the Er^{167} resonances below 118 eV. The theoretical curve is the Porter-Thomas function neglecting any possible difference in $\langle g\Gamma_n^0 \rangle$ for the two spin states.

For the region to 118 eV, we obtain $\Delta = 0.293$ vs $\Delta_{DM} = 0.533 \pm 0.22$ for two merged populations of nearly equal density, and 0.698 for two merged U.W. spacing distributions. The experimental value is even on the low side for the DM theory. Similarly, $\rho(S_j, S_{j+1}) = -0.309 \pm 0.169$. The value of $\rho(S_j, S_{j+1})$ for two merged populations is expected to be negative whether or not such correlation exists for each population separately. To test this, we performed Monte Carlo calculations mixing two populations (randomly), using level densities in the ratio 9 to 7. When the separate populations are "U.W.," we obtain $\rho(S_j, S_{j+1}) = -0.262 \pm 0.090$. When O.E. separate populations are used, we obtain $\rho(S_j, S_{j+1}) = -0.258 \pm 0.086$. The two theoretical results are essentially the same, and agree with the experimental result. Thus, no test of O.E. theory is provided by the experimental value of $\rho(S_j, S_{j+1})$.

E. Further Statistical Tests and Comments

Average s-Level Spacing $\langle D \rangle$

The evaluations of $\langle D \rangle$ of the preceding sections can, in principle, be made more precise by using an optimum statistic developed by DM.[2] This uses an energy interval $2L$ chosen such that levels need not be located at the ends of the interval. The weighting per level, f_j, is unity if it is near the middle of the interval, and decreases to zero according to a semicircle law at the ends of the interval. The evaluated quantity is

$$\langle D \rangle = (\pi L / 2W)(1 \pm 0.9/n),$$

where $W = \sum_j f_j$ and n is not too small. The value of $\langle D \rangle$ is mainly determined by the number of s levels believed to be in the interval. For Er^{166}, we obtain $\langle D \rangle = 38.4 \pm 0.32$, 38.4 ± 0.44, and 37.9 ± 0.43 eV, respectively, for the three choices displayed in Table XIII. The last value is lower, since the number of added s levels exceeds that of deleted p levels by one. The first two values agree, and are probably better choices in view of the somewhat arbitrary nature of the third choice. However, their associated uncertainties should be increased, since their n values may be in error by $\sim \pm 1$.

For Er^{168} we obtain $\langle D \rangle = 95.3 \pm 1.7$ eV for case A and 97.4 ± 1.8 eV for case B, where each stated uncertainty assumes that the n value is correct. Similarly for Er^{170}, cases C, D, E, and F give $\langle D \rangle = 155 \pm 5$, 159 ± 5, 160 ± 5, and 165 ± 5 eV, respectively. For Er^{167} to 118 eV, assuming that $n = 30$ is correct, we obtain $\langle D \rangle = 4.06 \pm 0.17$ eV, which has fractional uncertainty $1.27/n$ for two intermixed s populations. The actual uncertainties should be increased corresponding to the fact that the n values may be slightly in error for the s populations for the intervals.

Other Level-Spacing-Distribution Tests

In addition to Dyson's new F statistic test and Monahan and Rosenzweig's Λ statistic test, which are applied to these data in companion papers,[6,17] we consider two other tests.

(1) The first 100 spacings of Er^{166} have also been studied by subdividing the set into 10 nonintersecting subsets (each containing 10 adjacent level spacings), and forming the sums, S_{10}, of the 10 spacings of each subset. The expected distributions for $S_{10}/\langle S_{10} \rangle$ for the O.E. and U.W. were calculated by Monte Carlo methods and are shown in Fig. 12, along with the 10 observed values of 0.972, 1.058, 0.983, 1.004, 1.001, 1.105, 0.969, 0.795, 1.115, and 0.998. 6 of the 10 values deviate from unity by ≤ 0.031, which is small compared to the widths of either the O.E. or U.W. distributions. The overall standard deviation is $\sigma = 0.089 \pm 0.020$, vs 0.088 (O.E.) and 0.160 (U.W.). The experimental values favor the O.E. case.

(2) Recently Bohigas and Flores[19] (BF) have introduced the use of a statistic, which we denote as $\sigma(k)$, the mean standard deviation of the spacing

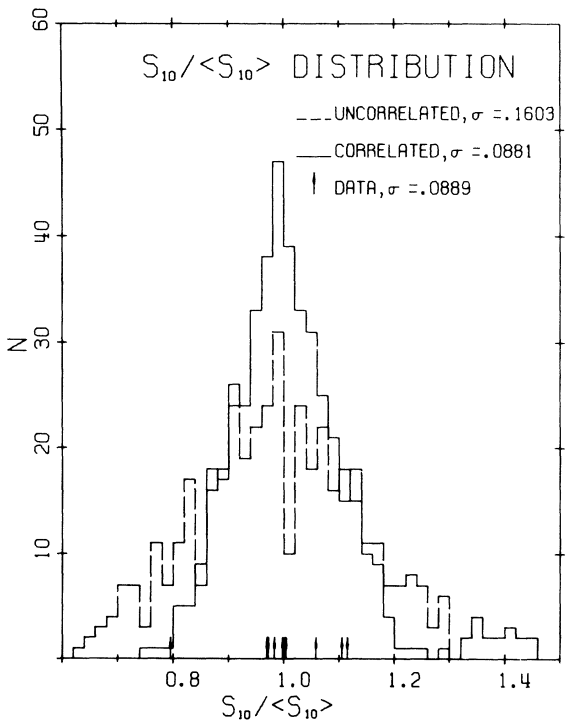

FIG. 12. The 10 values of $S_{10}/\langle S_{10} \rangle$ (as explained in the text) for the first 100 spacings of Er^{166} are indicated by the arrows. The histograms give the results of Monte Carlo calculations for sets of uncorrelated Wigner spacings, and for the random matrix model.

of levels having k levels between them in units of $\langle D\rangle$. Note that $k=9$ for Fig. 12 and $k=0$ is the nearest-neighbor case. Comparison with experiment for a given value of k uses $(E_{k+2}-E_1)$, $(E_{k+3}-E_2)$, $\ldots$, (E_n-E_{n-k-1}). They have used this test with older experimental results which do not provide pure and complete s populations. Those experimental $\sigma(k)$ values are larger than expected from O.E. theory. They and others[20] have done calculations on what BF call two-body random Hamiltonian ensembles (TBRE), which are supposed to approximate a situation that starts with single-particle shell-model states and then uses a small number of independent random variables which are supposed to approximate the two-body interaction. In the resulting $N\times N$ square matrices there are $\ll N(N+1)/2$ independent variables. The resulting spacing distributions seem to agree with the Wigner nearest-neighbor spacing law ($k=0$), but show even larger values for $\sigma(k)$ than for a U.W. spacing set for $k>0$. In Fig. 13 we show the BF $\sigma(k)$ vs k for their TBRE case, and those for the O.E. and U.W. cases from our Monte Carlo studies. The results for Er^{166} to 4.2 keV (all), Er^{168} (choice A), and Er^{170} (choice C) are also shown and are seen to agree best with the O.E. case. We also show the 10 and 90% limits for the O.E. case for $n=31$, 50, and 109. The similar calculations for Er^{168} (choice B) and Er^{170} (choices D, E, and F) were also made. These latter cases are not shown, but they agree about equally well with the O.E. case. While the experimental results seem to rule out their TBRE curve, we are not convinced that their calculations are sufficiently general that this disagreement implies that effective two-body forces are inadequate to generate results consistent with the O.E. case. Wigner has also emphasized this point.[21]

Tests Involving the Γ_n^0 Values

There are the obvious tests for the correlation coefficients for adjacent Γ_n^0 values and for the Γ_n^0 value and the average of the two nearest-neighbor spacings separated by that level. We denote these as $\rho(\Gamma_n^0, \Gamma_{nj+1}^0)$ and $\rho(\Gamma_n^0, S)$.

The experimental $\rho(\Gamma_n^0, S)$ values are all negative but near zero. They are individually consistent with zero. For the cases ordered as in Table XIII, we obtain the following values for $\rho(\Gamma_n^0, S)$: Er^{166}, -0.09 ± 0.08, -0.09 ± 0.10, -0.05 ± 0.11; Er^{168}, -0.09 ± 0.16, -0.06 ± 0.14; Er^{170}, -0.13 ± 0.15, -0.16 ± 0.15, -0.15 ± 0.15, and -0.15 ± 0.14. The $\rho(\Gamma_{nj}^0, \Gamma_{nj+1}^0)$ values are: Er^{166}, -0.21 ± 0.08, -0.28 ± 0.09, -0.25 ± 0.09; Er^{168}, -0.13 ± 0.15, -0.12 ± 0.14; Er^{170}, -0.20 ± 0.16, -0.35 ± 0.15, -0.27 ± 0.16, and -0.29 ± 0.16. The Er^{168} values are consistent with zero. The Er^{170} values are more than 1 standard deviation negative from zero, but are not convincingly inconsistent with zero. The Er^{166} values have the smallest standard deviation because of the larger sample sizes, and are negative by ~3 standard deviations from zero. The expected mean of $\rho(\Gamma_{nj}^0, \Gamma_{nj+1}^0)$ for not too small n is $\approx -1/n \pm 1/(n)^{1/2}$, for the case of no true correlation. The experimental values above are all systematically more negative than $-1/n$.

It has been customary to express the fractional uncertainty in a strength-function evaluation for an interval containing n s levels as $\pm 1.5/n^{1/2}$ due to statistical uncertainties. One assumes that the spacings form a U.W. set for which the contribution due to the fractional fluctuation in n for a given ΔE is $[(4-\pi)/\pi n]^{1/2}$. This part clearly disagrees with the O.E. prediction of about $\pm 1/n$. For a fixed n, if one assumes that the Γ_n^0 set is uncorrelated, but drawn from a common PT sin-

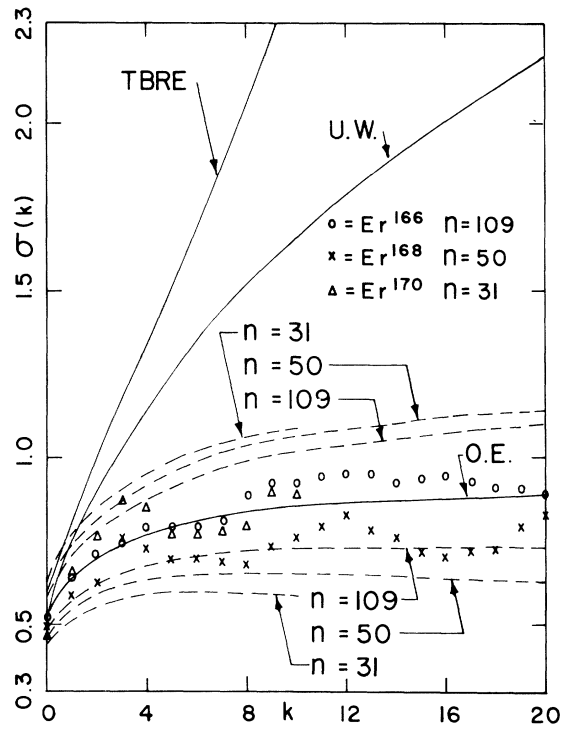

FIG. 13. Comparison of experimental erbium data for $\sigma(k)$ vs k with Monte Carlo results. Here $\sigma(k)$ is the standard deviation of $S(k)/\langle S(0)\rangle$, where $S(k)$ is the spacing of levels having k levels between them. The discrete data points shown correspond to the following cases: Er^{166}, all levels to 4.2 keV; Er^{168}, choice A of Table XIII; Er^{170}, choice C of Table XIII. The solid curves display the mean $\sigma(k)$ corresponding to the O.E., U.W., and Bohigas-Flores TBRE (Ref. 19) cases. The dashed curves give the 10 and 90% limits for the O.E. case, for 31, 50, and 109 levels.

gle-channel distribution having a common $\langle\Gamma_n^0\rangle$, the contribution from this is $\pm(2/n)^{1/2}$. The $\rho(\Gamma_{nj}^0, \Gamma_{nj+1}^0)$ values for Er^{166} suggest that a true negative correlation may exist. This would, if true, lead to a smaller contribution to the fractional uncertainty in S_0 from the Γ_n^0 values. As an additional test of this matter, we introduce a statistic which is similar to the DM Δ statistic, except the cumulative sum of $\Gamma_n^0/\langle\Gamma_n^0\rangle$ values replaces the cumulative level count $N(E)$:

$$\Delta_{S.F.} \equiv \min_{A,B} \frac{1}{\Delta E} \int_{E_0}^{E_0+\Delta E} \left[\frac{\sum \Gamma_n^0}{\langle\Gamma_n^0\rangle} - AE - B \right]^2 dE . \quad (8)$$

Figure 14 shows the experimental value of $\Delta_{S.F.}$ for Er^{166} to 4.2 keV, with the calculated probability of obtaining $\leq$ given values of $\Delta_{S.F.}$ for an uncorrelated set of PT-generated Γ_n^0 values having a common $\langle\Gamma_n^0\rangle$. This was done for U.W. level spacings and for equal level spacings. The O.E. case should lie closer to the equal spacing case

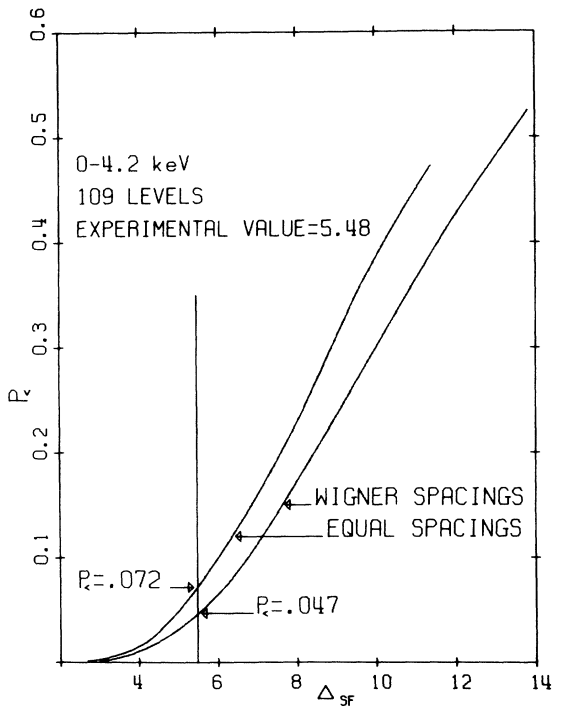

FIG. 14. The $\Delta_{S.F.}$ statistic is the mean square deviation between the staircase for $\sum\Gamma_n^0/\langle\Gamma_n^0\rangle$ and a best fitting straight line. The experimental value for the 109 levels of Er^{166} to 4.2 keV is shown along with the probability of obtaining this value or less for a set of uncorrelated adjacent Γ_n^0 values which have a Porter-Thomas distribution. The left curve is for a regular grid of level positions, while the right curve is for uncorrelated Wigner spacings. The case of levels following the Dyson theory will be between the two curves. This tests long-range order in the Γ_n^0 values.

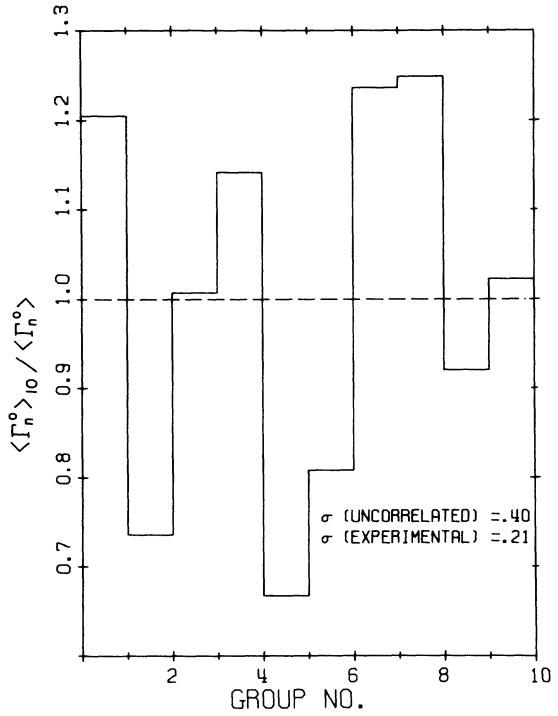

FIG. 15. A plot of $\langle\Gamma_n^0\rangle_{10}/\langle\Gamma_n^0\rangle$ for groups of 10 successive levels at a time for the first 100 levels of Er^{166}. This tests for long-range order in the Γ_n^0 values. For no correlations of adjacent widths which follow a Porter-Thomas distribution, a standard deviation of ± 0.40 is expected.

than to the U.W. case. The values $P_< = 0.047$ and 0.072 are so small that it seems unlikely that the Γ_n^0 values are uncorrelated.

A further test for regularity is provided by dividing the first 100 levels for Er^{166} into 10 adjacent, nonoverlapping groups of 10 levels [i.e., (1–10), (11–20), etc.] and using the 10-fold averages $\langle\Gamma_{n10}^0\rangle$, divided by the 100-fold average $\langle\Gamma_n^0\rangle$. The results are plotted in Fig. 15. This is similar to the treatment of the spacings in Fig. 12, except that the successive values are plotted vs group number. The experimental standard deviation, $\sigma = 0.21$, compares with $\sigma = 0.40$ for an uncorrelated set of (PT) Γ_n^0 values.

All of the above tests for the Er^{166} results suggest a short-range regularity of the Γ_n^0 values which has not been expected theoretically. We have no suggested explanation for this effect, if real, and welcome suggestions on the subject.

ACKNOWLEDGMENTS

We wish to thank Dr. George Rogosa and his colleagues at the AEC for help in procurement of the separated-isotope samples. Professor

W. W. Havens, Jr., is mainly responsible for seeing through the procurement of our new on-line computer and interface system. The interface system and other experimental electronics were developed by the Pegram Laboratory electronics group under Dr. Jack Hahn. Dr. Hugo Ceulemans, now returned to Mol, Belgium, made major contributions to preparing for and carrying out the measurements. He has taken responsibility for the analysis of the data for the separated Nd isotopes, obtained during the run. The contributions of the nonscientific members of our neutron velocity spectrometer group, Arthur Blake, Lester Morganstein, and William Van Wart, were important for the success of the experiments, as were those of others of the Nevis technical staff. We particularly thank Ann Terrien for typing the manuscript. The interest and encouragement provided by Professor Dyson, and by Dr. Rosenzweig and Dr. Monahan are gratefully acknowledged.

*Research supported in part by the U. S. Atomic Energy Commission.

†Present address: National Bureau of Standards, Gaithersburg, Md.

‡Present address: Brooklyn College, N.Y., N.Y.

[1]Earlier papers in this series: I, J. L. Rosen, J. S. Desjardins, J. Rainwater, and W. W. Havens, Jr., Phys. Rev. 118, 687 (1960), U^{238}; II, J. S. Desjardins, J. L. Rosen, W. W. Havens, Jr., and J. Rainwater, *ibid.* 120, 2214 (1960), Ag, Au, Ta; III, J. B. Garg, J. Rainwater, J. S. Petersen, and W. W. Havens, Jr., *ibid.* 134, B985 (1964), Th^{232}, U^{238}; IV, J. B. Garg, W. W. Havens, Jr., and J. Rainwater, *ibid.* 136, B177 (1964), As, Br; V, J. B. Garg, J. Rainwater, and W. W. Havens, Jr., *ibid.* 137, B547 (1965), Nb, Ag, I, Cs; VI, S. Wynchank, J. B. Garg, W. W. Havens, Jr., and J. Rainwater, *ibid.* 166, 1234 (1968), Mo, Sb, Te, Pr; VII, J. B. Garg, J. Rainwater, and W. W. Havens, Jr., to be published.

[2]The series of papers by Dr. Dyson alone, and with Dr. Mehta are as follows: F. J. Dyson, J. Math. Phys. 3, 140, 157, 166, 1199 (1962), denoted I, II, III, and T. F. W.; and M. L. Mehta and F. J. Dyson, *ibid.* 4, 701, 713 (1963), denoted IV and V. (These papers are republished in Ref. 3.)

[3]C. E. Porter, *Statistical Theories of Spectra Fluctuations* (Academic, New York, 1965) has reprints of essentially all published and many unpublished papers on this subject up to early 1964. See also Refs. 4, 5.

[4]C. E. Porter and R. G. Thomas, Phys. Rev. 104, 483 (1956).

[5]C. f. the review article by A. M. Lane and R. G. Thomas, Rev. Mod. Phys. 30, 257 (1958).

[6]H. I. Liou, H. S. Camarda, and F. Rahn, following paper, Phys. Rev. C 5, (1972).

[7]J. Rainwater, W. W. Havens, Jr., J. S. Desjardins, and J. L. Rosen, Rev. Sci. Instr. 31, 481 (1960).

[8]J. Rainwater, W. W. Havens, Jr., and J. B. Garg, Rev. Sci. Instr. 35, 263 (1964).

[9]S. F. Mughabghab, R. E. Chrien, and M. R. Bhat, Phys. Rev. 162, 1125 (1967).

[10]C. f. G. Michaud, L. Scherk, and E. Vogt, Phys. Rev. C1, 864 (1970).

[11]M. L. Mehta, *Random Matrices and the Statistical Theory of Energy Levels* (Academic, New York, 1967).

[12]M. Gaudin, Nucl. Phys. 25, 447 (1961).

[13]M. L. Mehta and J. des Cloizaux, to be published.

[14]H. S. Camarda, Ph.D. thesis, Columbia University, 1970 (unpublished).

[15]F. J. Dyson, J. Math. Phys. 3, 1191 (1962).

[16]J. E. Monahan and N. Rosenzweig, Phys. Rev. C 1, 1714 (1970).

[17]J. E. Monahan and N. Rosenzweig, Phys. Rev. C 5, 1078 (1972).

[18]L. M. Bollinger and G. E. Thomas, Phys. Rev. 171, 1293 (1968).

[19]O. Bohigas and J. Flores, in Proceedings of the International Conference on Statistical Properties of Nuclei, Albany, New York, 1971, to be published.

[20]O. Bohigas and J. Flores, Phys. Letters 34B, 261 (1971); 35B, 383 (1971); J. B. French and S. S. M. Wong, *ibid.* 33B, 449 (1970); 35B, 5 (1971).

[21]E. P. Wigner, Round Table Discussion of Selected Topics, International Conference on Statistical Properties of Nuclei, Albany, New York, 1971, to be published.